HIGH TEMPERATURE DIELECTRIC RELAXATION OF POLY (VINYLIDENE FLUORIDE)

1976

SHIGEYOSHI OSAKI

Department of Polymer Science
Faculty of Science
Osaka University

High Temperature Dielectric Relaxation

of

Poly(vinylidene Fluoride)

A Doctoral Thesis Submitted by

Shigeyoshi Osaki

to the Faculty of Science, Osaka University

1976

Acknowledgements

This work was performed at the Laboratory of Polymer Physics, Faculty of Science, Osaka University. I am much indebted to Assistant Professor Yoichi Ishida, who suggested the subject, promoted the research, and gave me continuing guidance, advice, and encouragement. I am deeply indebted to Mr. Shinsaku Uemura and to Dr. Keiichiro Adachi for their kind guidance, and to Professor Hiroshi Fujita and Assistant Professor Akio Teramoto for a critical reading of the manuscript. Thanks are also due to Professor Hiroyuki Tadokoro, Dr. Masamichi Kobayashi, and the members of Tadokoro's Laboratory for their kind discussion, and due to Dr. Masahiro Mori and Dr. Makoto Kaburagi at the Department of Physics for their frank discussion and friendship, and Assistant Professor Shinsuke Yamashita of Tokushima University for his continuing encouragement. My gratitude is also rendered to Assistant Professor Yu Yokoyama for his help with emission spectroscopy, to Mr. Takashi Tagawa and Mr. Masaru Kashima of Unitika Co., Ltd. for the use of a small-angle X-ray diffractometer, and to Dr. Haruko Kakutani of Kureha Chemical Co., Ltd. for providing the poly(vinylidene fluoride) sample used. My thanks go to all the members of the Laboratory of Polymer Physics in Osaka University for their kindness and encouragement. Finally, it is a pleasure to acknowledge the assistance of Miss Toshiko Hino in the typewriting.

Contents

Introduction

Like mechanical measurements and nuclear magnetic resonance spectroscopy, dielectric measurements over ranges of frequency and temperature provide data which are basic to elucidating various modes of molecular motions in polymeric solids, though their applicability is limited to polar substances. This type of experiment is usually performed in two ways: in one of them the real and imaginary parts, denoted commonly by ε' and ε'', of the complex dielectric constant $\varepsilon^* = \varepsilon' - i\varepsilon''$ ($i = \sqrt{-1}$) are measured as a function of frequency at fixed temperatures, and in the other both ε' and ε'' are measured as a function of temperature at fixed frequencies. Resulting values of ε' and ε'' give either a dielectric frequency or a dielectric temperature relaxation curve, depending on whether they are plotted against frequency or temperature. Both types of curves are equally important for the investigation of molecular motions in solids. Since the pioneering work by Fuoss and Kirkwood[1-3] about thirty years ago, such relaxation curves have been determined for a great many polymers, both essentially amorphous and partially crystalline, and efforts have been made to correlate the observed relaxations with the molecular motions in particular polymers under investigation.[4] As far as essentially amorphous polymers are concerned, such efforts have reached a fairly satisfactory stage, and we now know that dielectric relaxations of amorphous polymers arise from both long-ranged and short-ranged motions of the main chains as well as local motions of the side chains.

Crystalline polymers present a more complex, but a more interesting situation. In them, in addition to these contributions from the amorphous part, there appear dielectric relaxations which are to be associated with the molecular motions inside the crystalline region and on its surface, i.e., the boundary between the amorphous and crystalline regions. Evidently, these motions ought to be certain reflections of the molecular arrangement, i.e., the geometrical structure, of the crystalline region of a particular polymer.

Poly(vinylidene fluoride)(PVDF) is a polar polymer of simple chemical structure and can be crystallized, though partially, into three different modifications called form I, form II, and form III.[5-8] These features of PVDF make it a useful sample for investigating by dielectric analysis how the molecular motions are affected by the crystal structure in which the long chain molecules are geometrically arranged. The study reported in this thesis deals with dielectric relaxations of forms II and III PVDF in the region of temperatures encompassing their melting points. Form I PVDF is not considered because it has a crystal structure quite similar to that of form III PVDF. It is one of the features of PVDF that it shows marked dielectric relaxations at temperatures near its melting point, and one may expect that these relaxations should be a sensitive function of the structure of its crystalline portions. This expectation and the fact that no experimental study had been reported to substantiate it motivated the author to launch the experimental work described below. In the ensuring presentation, the dielectric relaxation observable with a crystalline polymer at temperatures near its melting point is distinguished from those which may be found at lower temperatures by the term

"high temperature relaxation." It is to be noted that, apart from PVDF,[9-11] the high temperature relaxation has so far been observed only with oxidized polyethylene[12-18] and poly(chlorotrifluoroethylene).[19] For form II PVDF this type of dielectric relaxation has been investigated in detail by several authors, but little has been done with either form I or form III PVDF. In this point the present experiment with form III PVDF may claim its scientific value.

In the description that follows, the PVDF samples prepared so as to obtain crystalline forms I, II and III are simply referred as forms I, II and III PVDF.

Form II PVDF ($P2_1/c$) can be prepared by quenching the melt, and it consists of the molecular chains of $TG\bar{T}\bar{G}$ type.[8] Form II PVDF thus obtained presents no difficulty in dielectric measurements at high temperatures. Form I PVDF (Cm2m) can be prepared by the stretching method, and form III PVDF (C121) by the solvent casting.[8] Both are such polar crystals in which the molecular chains are in planar zigzag conformation and have the dipole moments that are perpendicular to the molecular axis and do not cancel one another. However, form I and form III PVDF obtainable by these conventional methods are not suitable for the study of the high temperature dielectric relaxation. As the temperature approaches the melting point, form I PVDF undergoes appreciable shrinkage and form III PVDF is disturbed by anomalously large ionic conduction. A greater part of the present work was thus devoted to finding the preparative conditions for form III PVDF which would allow satisfactory measurements to be made in the vicinity of the melting temperature, and the author indeed found that the desired samples could

be prepared by isothermal crystallization from the melt. The discovery of this fact was crucial for the present work, because it made the entire project carry through. The method of isothermal crystallization was also very useful for the preparation of form II PVDF adequate for high temperature dielectric measurements.

Chapter 1 of the text describes in detail the methods used for measurements of necessary physical quantities and the original samples of PVDF employed for the present study.

Chapter 2 is concerned with the preparation of form II and form III PVDF by the isothermal crystallization method. Effects of the time and temperature on annealing and crystallization are examined in detail to find the optimum conditions.

The low frequency dielectric behavior of untreated PVDF at high temperatures is accompanied with the conduction of ions contained as impurities in the sample. Chapter 3 describes efforts to minimize this effect so that the high temperature dielectric relaxation truly associated with the polymer itself may be observed.

Although there exists rather definitive evidence showing that the high temperature relaxation of form II PVDF is attributable to the molecular motions in the crystalline region,[9-11] some authors[20-22] are still of opinion that the amorphous region should be responsible for them. In Chapter 4 we give further experimental evidence against the latter view.

Chapter 5 is devoted to the high temperature relaxation of form III PVDF. The data obtained are compared with those for form II PVDF and interpreted in terms of molecular concepts.

Principal results and conclusions from the present investigation are summarized in Chapter 6.

References

1. R. M. Fuoss, J. Am. Chem. Soc., 60, 451 (1938).
2. R. M. Fuoss and J. G. Kirkwood, J. Am. Chem. Soc., 63, 385 (1941).
3. J. G. Kirkwood and R. M. Fuoss, J. Phys. Chem., 9, 329 (1941).
4. N. G. McCrum et al., " Anelastic and Dielectric Effects in Polymer Solids," John Wiley and Sons, London-New York (1967).
5. T. B. Lando, H. G. Olf, and A. Peterlin, J. Polym. Sci., A-1, 4, 941 (1967).
6. G. Cortili and G. Zerbi, Spectrochim. Acta., 32A, 2216 (1967).
7. R. Hasegawa, M. Kobayashi, and H. Tadokoro, Polymer J., 3, 591 (1972).
8. R. Hasegawa, Y. Takahashi, Y. Chatani, and H. Tadokoro, Polymer J., 3, 600 (1972).
9. H. Sasabe, S. Saito, M. Asahina, and H. Kakutani, J. Polymer. Sci., A-2, 7, 1405 (1969).
10. S. Yano, J. Polym. Sci., A-2, 8, 1057 (1970).
11. K. Nakagawa and Y. Ishida, J. Polym. Sci., A-2, 11, 1503 (1973).
12. W. G. Oakes and D. W. Robinson, J. Polym. Sci., 14, 505 (1954).
13. G. P. Mihailov, S. P. Kabin, and B. I. Sazhin, Zhur. Tekh. Fiz., 25, 590 (1955).
14. S. Okamoto and K. Takeuchi, J. Phys. Soc. Japan, 14, 378 (1959).
15. S. Saito and T. Nakajima, J. Polym. Sci., 36, 533 (1959).
16. W. Reddish and J. T. Barrie, paper presented at the IUPAC International Symposium on Macromolecular Chemistry (1959).
17. C. A. F. Tuijinman, Polymer, 4, 259, 315 (1963).
18. Y. Ishida and K. Yamafuji, Kolloid-Z., 202, 26 (1955).

19. A. H. Scott, D. J. Scheiber, A. J. Curtis, J. I. Lauritzen, and J. D. Hoffman, J. Rev. Nat. Bur. Stand., 66A, 269 (1962).

20. R. F. Boyer, private communication.

21. D. R. Paul and J. O. Altamirano, Amer. Chem. Soc., Div. Polymer Chem., Reprints, 15(1), 409 (1974).

22. Jen Ciu, private communication.

Chapter 1

Experimental Details

1-1. Introduction

Experimental study of the physical properties of a polymeric substance requires samples that can be well characterized. In the present work, the samples of PVDF used were characterized by density measurements, infrared and X-ray analyses, and differential scanning calorimetry. They were subjected not only to dielectric measurements but also to measurements of dc conductivity, P-E hysteresis loop, and mechanical relaxation. The samples and the experimental methods used are described below.

1-2. Experimental Methods

1-2-1. Density

Densities were measured at 25°C by the flotation method with ethylene dibromide and carbon tetrachloride as confining liquids. Temperature of the water bath was regulated to within $\pm$ 0.05°C.

1-2-2. Infrared Spectroscopy

Infrared spectra from 4000 to 400 cm^{-1} were taken with a DS-402G infrared spectrophotometer of Japan Spectroscopic Co., Ltd. Far-infrared spectra from 400 to 30 cm^{-1} were taken with a Hitachi FIS-3 spectrophotometer. These measurements at high temperatures were made by sandwiching a specimen between KBr disks, and the temperature was measured by a thermocouple. The temperature was regulated to within $\pm$ 1°C by using a thermostat.

1-2-3. X-ray Diffraction

X-ray diffraction patterns were obtained by a Model MJ 200 AN (Rigaku Denki) equipped with a proportional counter. Nickel-filtered CuKα radiation (wavelentgh: 1.542 Å) was used. The crystal form of a specimen was judged from X-ray diffraction patterns taken by a flat camera. The measurements at high temperatures were carried out by blowing hot air over the specimens. The tempereture of blowing air was regulated to within ±1°C. The diffraction intensities were recorded at various fixed temperatures. The degree of crystallinity was determined by Gal'perin's method.[1] Small-angle X-ray photographs were taken on a Rigaku Denki small-angle X-ray diffractometer and the long period was determined with collagen as a reference substance.

1-2-4. Differential Scanning Calorimetry (DSC)

A model 8055 (Rigaku Denki) differential scanning calorimeter was used. The heating rate was regulated to 10°C/min, and the temperature was calibrated with indium and tin standards. The melting temperature T_m of the sample was determined from the peak of the DSC curve. The enthalpy relating to the melting was estimated from the area of the DSC curve above the base line.

1-2-5. Dielectric Measurements in the Audio Frequency Region

The real and imaginary parts, denoted by ε' and ε", of the complex dielectric constant were measured by a mutual inductance bridge[2,3] over the frequency range from 6 Hz to 1.6 MHz at various temperatures. The circuit diagram is shown in Figure 1.1. An oscilloscope was used as the detector of the bridge.

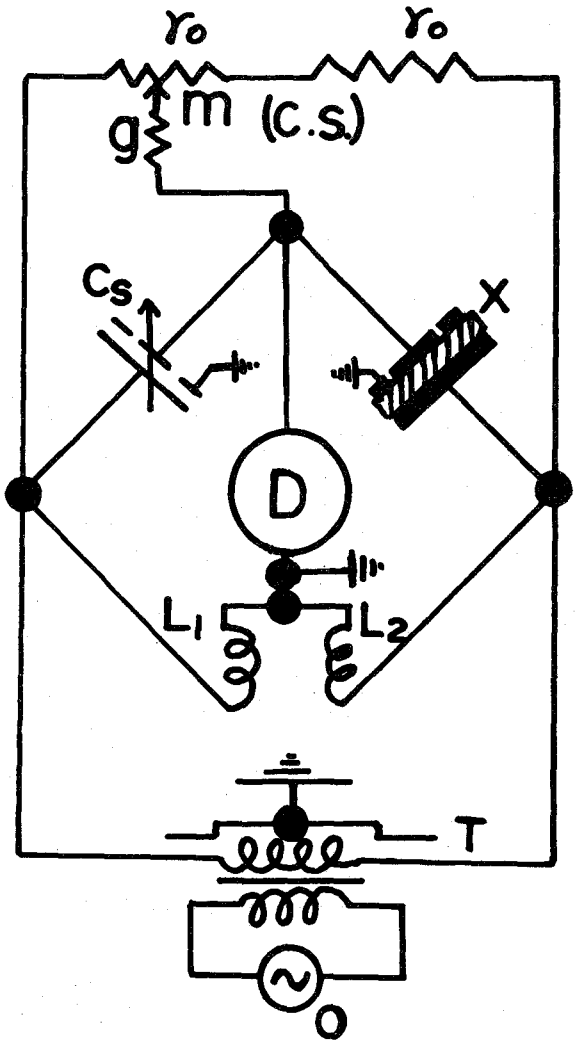

Figure 1.1. Inductive-ratio-arm bridge. (X) sample; (C_s) variable air condenser; (L_1, L_2) inductive ratio arm; (C.S.) conductance shifter; (r_o, g) resistor; (m) contactor; (T) shielded transformer; (O) oscillator; (D) detector.

The specimens coated with evaporated gold or silver were connected to the measuring arms of the bridge. When the conductance and capacitance reached balance, reading was taken on the variable condenser and conductance shifter. The values of ε' and ε'' of the specimen were calculated from

$$\varepsilon' = C_s / C_o \tag{1-1}$$

$$\varepsilon'' = G_s / 2\pi f C_o \tag{1-2}$$

where C_o is the geometrical capacitance of the electrode, C_s is the capacitance obtained from readings of the variable condenser, G_s is the conductance obtained from readings of the conductance shifter, and f is frequency.

The cell used had been designed in our laboratory. It is diagrammatically shown in Figures 1.2 and 1.3. The vessel for loading a given specimen is made of brass and sealed from open air by a silicone rubber packing. To eliminate effects of oxidation or humidity upon the specimen, the inner air was replaced by dry nitrogen. Guarded, unguarded, and guard electrodes were mounted in the vessel, as shown in Figure 1.3. In order to reduce the errors resulting from residual inductances and resistances at higher frequencies, coaxial cables were used for connecting the guarded and unguarded electrode plates to the connector terminals. Stray capacitances were eliminated by using the guard electrode. The temperature was regulated to within $\pm$ 0.1°C. Values of the complex dielectric constant were determined in this way to the accuracy of $\pm$ 3%.

The same cell was also used for measurements of other electric properties which are described below.

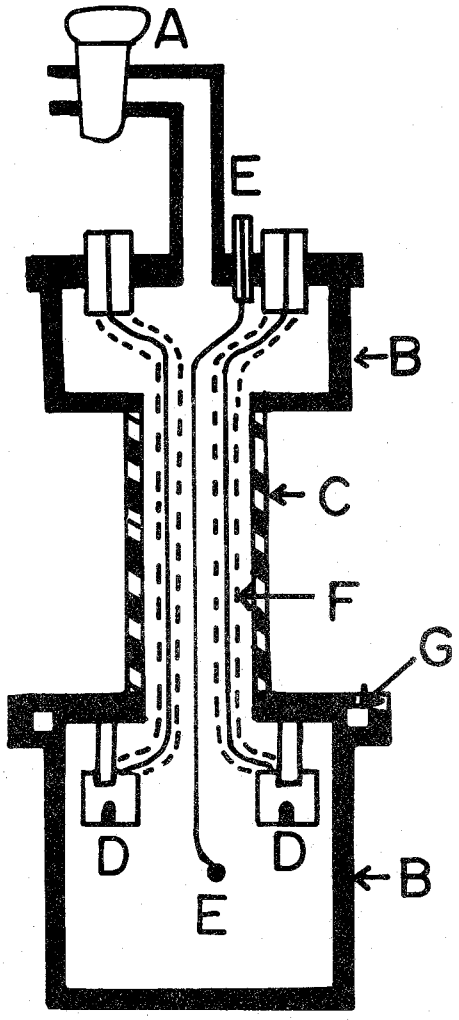

Figure 1.2. Air-tight vessel. (A) vacuum cock; (B) brass; (C) stainless pipe; (D) co-axial connector; (E) thermocouple; (F) co-axial cable; (G) silicone rubber "O" ring.

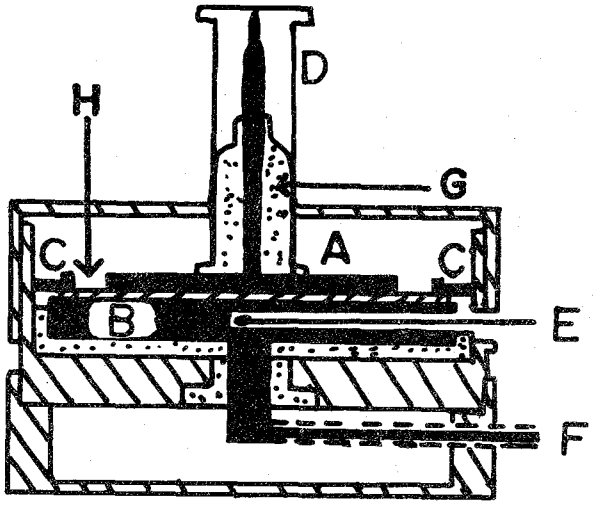

Figure 1.3. Three-terminal guarded-electrode cell. (A) guarded electrode; (B) unguarded electrode; (C) guard electrode; (D) co-axial connector; (E) thermocouple; (F) co-axial cable; (G) teflon; (H) specimen.

1-2-6. Dielectric Measurements under DC Bias

Dielectric measurements under dc bias were also carried out over the frequency range from 30 Hz to 20 KHz by means of a modified mutual inductance bridge,[4,5] which is shown in Figure 1.4. A battery for the bias was connected in series between the detection terminal of the bridge and the ground through a protecting resistor (R) chosen so that its resistance was much smaller than the dc resistance of the specimen. The dc current through the conductor was shut off by inserting a condenser between the conductor and the detection terminal.

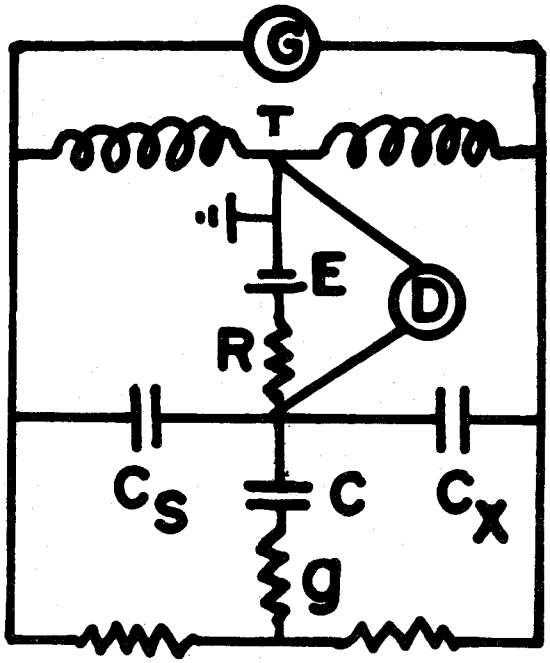

Figure 1.4. Mutual inductance bridge for dielectric measurements under dc bias. (G) generator; (T) transformer for rating arms; (E) battery for dc bias; (R) protecting resistor; (C) condenser for cutting off the dc current through the conductor g; (D) detector; (C_s) variable air condenser; (C_x) sample.

1-2-7. Dielectric Measurements in the Ultra-Low Frequency Region

An operational amplifier bridge for ultra-low frequencies from

10^{-2} Hz to 10^{2} Hz, designed originally by Irie,[6] was constructed by Uemura.[7] Figure 1.5 shows its circuit diagram. The bridge can be balanced by simple operations since it does not requires a Wagner ground.

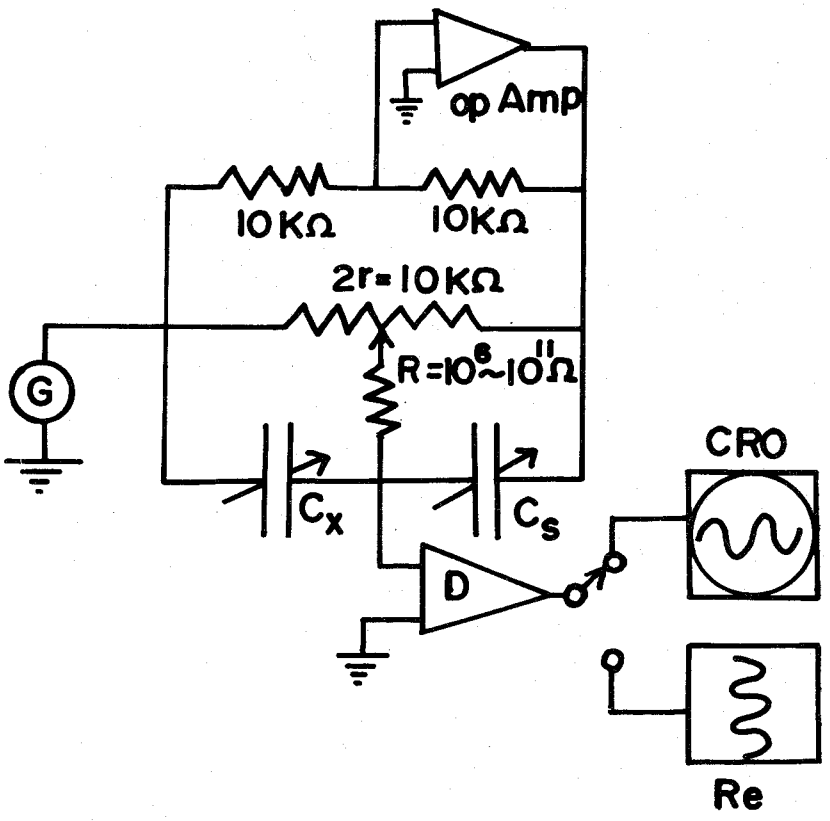

Figure 1.5. Circuit diagram of bridge for dielectric measurements in the ultra-low frequency region. (op Amp) operational amplifier with high input impedance; (G) ultra-low frequency generator; (D) null detector; (CRO) cathode ray oscilloscope; (Re) recorder; (C_s) standard air capacitor; (C_x) unknown capacitor; (2r, R) conductance shifter; The out put of detector D is viewed on CRO at frequencies above 3 Hz and is recorded with Re below 3 Hz.

1-2-8. DC Conductivity

Measurements of dc conductivity was made by applying a dc field at a fixed temperature, with a Keithley 640 vibrating capacitor electrometer being used.

1-2-9. P-E hysteresis Loop

P-E hysteresis loops at a frequency of 0.1 Hz were measured by the Sawyer-Tower method.[8] Figure 1.6 shows a circuit diagram for the measurement. A specimen of capacitance C_x was connected in series with a polystyrene condenser of capacitance C_o. When the applied voltage V is divided into a voltage V_x across the specimen and a voltage V_o across the polystyrene condenser, one obtains

$$V = V_x + V_o = V_x(1 + V_o / V_x) \qquad (1\text{-}3)$$

Since the surface charge of the specimen, Q, is equal to that of the polystyrene condenser, one can write

$$Q = C_x V_x = C_o V_o \qquad (1\text{-}4)$$

so that

$$C_x / C_o = V_o / V_x \qquad (1\text{-}5)$$

Polarization P, which is equal to charge per unit area, is proportional to V_o by equation (1-4). If C_x/C_o is much smaller than unity, V_x becomes nearly equal to the applied voltage V by equations (1-3) and (1-5).

Thus, the P-E hysteresis loop was obtained from a plot of V_o against V. The X-Y recorder had ordinates proportional to V_o and abscissae proportional to V.

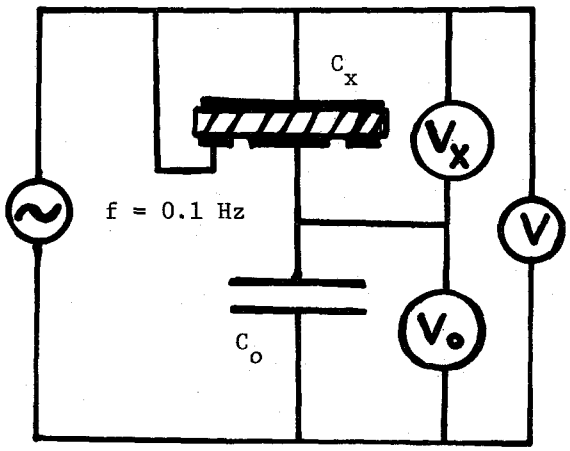

Figure 1.6. Schematic diagram for measurement of P-E hysteresis loop. (C_x) capacitance of specimen; (C_o) capacitance of polystyrene condenser; (V) applied voltage; (V_x) voltage across specimen; (V_o) voltage across polystyrene condenser.

1-2-10. Mechanical Measurements

Dynamic viscoelastic properties were measured by a direct reading dynamic viscoelastometer of Toyo Measuring Instrument Co., Ltd., Vibron DDV-II .[9] The specimens for these measurements were 0.1 mm thick, 2.5 mm wide, and about 20 mm long. Measurements were made at 3.5 Hz over the range from room temperature to 190°C with a constant rate of heating, 1.5°C/min. Tangent δ was read directly from the meter, and the storage tensile modulus E' was calculated from the dial reading and the size of the specimen. Loss tensile modulus E" was calculated from E' and tan δ.

1-2-11. Emission Spectroscopy

In order to identify the species of ions contained in the samples emission spectra were taken by using a Shimazu QF-60 Emission Spectrophotometer.

1-3. Materials

A PVDF powder called KF-Polymer was kindly supplied by Dr. H. Kakutani of Kureha Chemical Co., Ltd. The number-average degree of polymerization was stated to be approximately 1000. Another PVDF powder called Kynar was kindly supplied by Dr. J. Gall of Pennsalt Co., Ltd.

These powders were dissolved in purified acetone, and the solution was added dropwise onto distilled water. The precipitated PVDF was collected on a glass filter and dried under vacuum. This treatment for purification was repeated twice.

Dielectric studies of PVDF had been made with KF-Polymer as sample in Japan and with Kynar as sample in U. S. A. This difference in sample introduced a confusion into the assignment of the high temperature relaxation. In order to clarify the causes of the confusion, we felt necessary to characterize these two samples, and determined the contents of "head-to-head" bonding in them from NMR measurements using a Varian XL-100 NMR spectrometer. Tetramethylsilane was used as a reference substance for determining chemical shifts. The content of "head-to-head" bonding in KF-Polymer was about 8% when calculated from ^{19}F (94.1 MHz) spectra in a mixture of dimethyl acetamide and deuterated acetone, and the corresponding content in Kynar was about 14%.

References

1. Ye. L. Gal'perin, B. P. Kosmynin, and V. K. Smirov, Vysokomol. Soed., 8, 1880 (1970).
2. R. H. Cole and P. M. Gross, Rev. Sci. Instr., 20, 252 (1949).
3. Y. Ishida, Kolloid-Z., 168, 29 (1960).
4. S. Osaki, S. Uemura, and Y. Ishida, Rept. Progr. Polym. Phys. Japan, 8, 403 (1970).
5. S. Uemura, J. Polym. Sci., A-2, 10, 2155 (1972).
6. H. Inomata and F. Irie, Technol. Repts. Kyushu Univ., 37, 330 (1964).
7. S. Uemura, J. Polym. Sci., A-2, 12, 1177 (1974).
8. C. B. Sawyer and C. H. Tower, Phys. Rev., 35, 269 (1930).
9. M. Takayanagi, Mem. Fac. Eng. Kyushu Univ., 23, 41 (1963).

Chapter 2

Effects of Annealing and Isothermal Crystallization upon Crystalline Forms of Poly(vinylidene Fluoride)

2-1. Introduction

Kondrashov[1] and Makarevich and Nikitin[2] found by X-ray diffraction and infrared spectroscopy that poly(vinylidene fluoride)(PVDF) can exist in two crystalline forms. Okuda et al.[3] showed by infrared spectroscopy and electron diffraction that PVDF can crystallize in two forms α and β from dilute solution. Gal'perin and Kosmynin,[4] Natta et al.,[5] and Lando et al.[6,7] confirmed the existence of the two crystalline forms, which Lando et al. designated I and II instead of β and α. The existence of a third form III was suggested by Cortili and Zerbi[8] from a study with films cast from dimethyl sulfoxide solution. Hasegawa et al.[9] studied the formation of these three crystalline forms and the transitions among them under high pressure. They found that form II can be obtained by crystallization from the melt, form I by stretching a melt-crystallized sample, and form III by crystallization under high pressure. Nakagawa and Ishida[10] investigated effects of annealing on form II by means of differential scanning calorimetry and electron microscopy.

Forms I and III are what are called polar crystals.[9] In either form, the molecular chains have planar zigzag conformation and the dipole moments are perpendicular to the molecular axis and do not cancel each other. Hence it can be expected that form I and form III should show some characteristic electric properties.

Form I PVDF sample has so far been prepared by the stretching method, and form III PVDF sample has been prepared by solvent casting as mentioned above. However, we found that the samples so prepared were not suitable for the study of dielectric behavior at high temperatures, because form I sample obtained by the stretching method underwent large thermal contraction and because form III sample obtained by the solvent-casting method showed anomalously large ionic contributions as the temperature was raised.

After a good many efforts for obtaining form III PVDF appropriate for dielectric measurements at high temperatures, we have found that the desired sample can be prepared by annealing or isothermal crystallization at temperatures between 165 and 185°C. This finding enabled us to establish the conditions under which it can be preferentially formed.

2-2. Experimental

2-2-1. Preparation of Specimens for X-ray Diffraction and IR Spectroscopy

Form II (MQ) The purified powder of KF-Polymer was moulded to a film between metal plates at 210°C, and the film was quenched into liquid nitrogen. The films thus formed were almost in form II, according to the X-ray photographs and IR spectra, and the density was 1.767g/cm^3 at 25°C. They were called form II (MQ).

Form II (SGC) Crystals were allowed to grow from an 0.1% KF-Polymer solution in a mixture (9:1 weight) of monochlorobenzene and dimethylformamide by slow cooling from the boiling temperature. These were collected on a glass filter and dried at room temperature under vacuum for two weeks. No residue of solvent remained in the crystal mat when detected by infrared spectroscopy. IR spectra showed that the solution-

grown crystal mats were also in form II. The density was 1.815g/cm^3 at 25°C. The specimens prepared in this way were referred to as form II (SGC).

Form III (SVT) Solvent cast films were prepared by evaporating solvent very slowly at 50°C from an 0.1% dimethylformamide solution of KF-Polymer. They were immersed in carbon disulfide at room temperature for three days and then dried at 50°C under a reduced pressure of 10^{-5}mmHg for three days. The specimens thus prepared, designated as form III (SVT) here, were found to be in form III by infrared spectroscopy.

2-2-2. Determination of Fractions of Different Crystalline Forms by Infrared Spectroscopy

The relative amounts of form II and form III in a given PVDF specimen were determined by using infrared absorption bands near 500 cm^{-1}: one at 530 cm^{-1} characteristic of form II and another at 510 cm^{-1} characteristic of form III.[3,9]

If these absorpotions are assumed to follow the Lambert-Beer law and not to interfere with each other, the absorbances D_{II} (at 530 cm^{-1}) and D_{III} (at 510 cm^{-1}) for a specimen of thickness L may be given by

$$D_{II} = \log (I^{\circ}_{II} / I_{II}) = K_{II} C_{II} L \qquad (2\text{-}1)$$

$$D_{III} = \log (I^{\circ}_{III} / I_{III}) = K_{III} C_{III} L \qquad (2\text{-}2)$$

where the subscripts II and III refer to form II and form III, respectively. Here I°_{II} and I°_{III} are the intensities of the incident radiation, I_{II} and I_{III} are the intensities of the transmitted radiation, K_{II} and K_{III} are the

absorption coefficients, and C_{II} and C_{III} are the molar concentrations of monomer units in the respective crystalline forms.

In terms of the degrees of crystallinity X_{II} and X_{III} of form II and form III, eqs.(2-1) and (2-2) may be rewritten

$$D_{II} = K_{II} C^{\circ} X_{II} L \tag{2-3}$$

and

$$D_{III} = K_{III} C^{\circ} X_{III} L \tag{2-4}$$

where C° in the average total monomer concentration in the sample.

The relative fraction F(III) of form III in the sample is given by

$$F(III) = C_{III} / (C_{III} + C_{II}) \tag{2-5}$$

We solve eqs.(2-1) and (2-2) for C_{II} and C_{III}, respectively, and subsitute them into eq.(2-5) to obtain

$$F(III) = \frac{D_{III}}{D_{III} + (K_{III} / K_{II}) D_{II}} \tag{2-6}$$

In order to use this equation for the determination of F(III), we must measure D_{II} and D_{III}, and moreover must know the ratio K_{III}/K_{II}. This was done in the following way.

Infrared spectra were taken on specimens of varying thicknesses; a typical example is illustrated in Figure 2.1. From such spectra, values

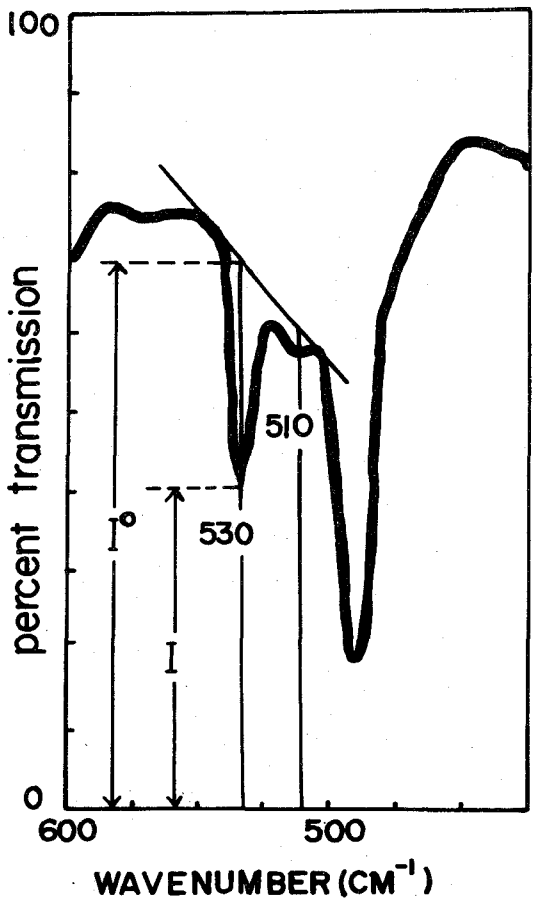

Fig. 2.1. Infrared spectrum of a form II (MQ) specimen and the base line.

of D_{II} and D_{III} were determined by drawing the base line to the spectrum in such a way that the Lambert-Beer law would be obeyed, i.e., D_{II} and D_{III} would be proportional to the film thickness. Figure 2.2 shows the results from such analyses, in which both D_{II} and D_{III} are seen to vary linearly with film thickness.

Estimation of K_{II} was made from D_{II} and X_{II} of a film quenched from the melt, which gave only a faint absorption at 510 cm^{-1}. A form III (SVT) film was used for K_{III}, since it exhibited no absorption band at 530 cm^{-1}. The values of X_{II} and X_{III} were determined by the X-ray counter method.[11] The value of C° was calculated to be 0.0305 mole/cm^3 by using the mean value of the crystal densities of form II (1.925 g/cm^3) and form III (1.973 g/cm^3).[9] These values together with the observed D_{II} and D_{III} were substituted into eqs.(2-3) and (2-4) to obtain $K_{II} = 10.0 \times 10^3$ cm^2/mole and $K_{III} = 8.1 \times 10^3$ cm^2/mole. Use of the K_{II} and K_{III} values thus obtained in eq.(2-6) gives

$$F(III) = \frac{D_{III}}{D_{III} + 0.81D_{II}} \qquad (2\text{-}7)$$

In actual analyses, values of F(III) were estimated from IR data taken at room temperature, because far-infrared spectra above 160°C could not be analyzed quantitatively due to great fluctuations of the background level. Therefore, the values of F(III) determined in this way may have been affected by the crystallization that would have occurred during the period of cooling.

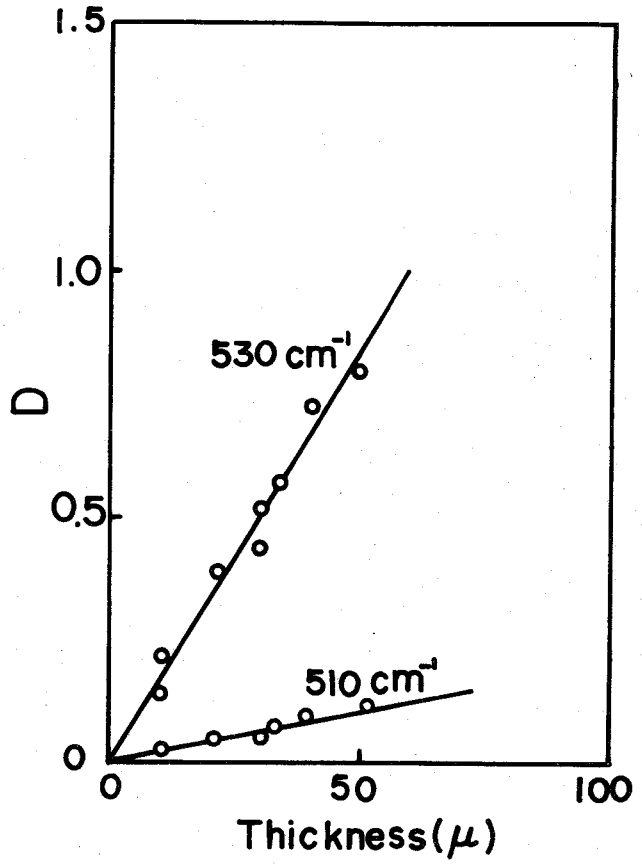

Fig. 2.2. Relation between the absorbances at 530 cm^{-1} (form II) and 510 cm^{-1} (form III) and film thickness.

2-2-3. Determination of the Equilibrium Melting Temperature

The equilibrium melting temperature T_m° was determined by the method of Hoffman and Weeks.[12] In this method, observed melting temperatures T_m are plotted against crystallization temperatures T_c, and the intersection of the extension of the plot with the line $T_m = T_c$ is taken to be the desired equilibrium melting temperature. The crystallization temperature were measured by a thermocouple placed near the specimen.

2-3, Results and Discussion

2-3-1. Annealing of Solution-Grown Crystal Mats

The IR spectra in Figure 2.3 show that annealing at 185.8°C for 20 hr caused form II to transform to form III. The time dependence of this transformation is illustrated in terms of F(III) in Figure 2.4, which indicates that the fraction of form III, F(III), approaches an asymptotic value in about 20 hr.

Effects of annealing temperature upon F(III) were investigated with form II (SGC) annealed at different temperatures for 20 hr. Figure 2.5 shows the results. It is seen that F(III) starts increasing at about 175°C, reaches a maximum of 0.9 at 185°C, and finally decreases above 190°C.

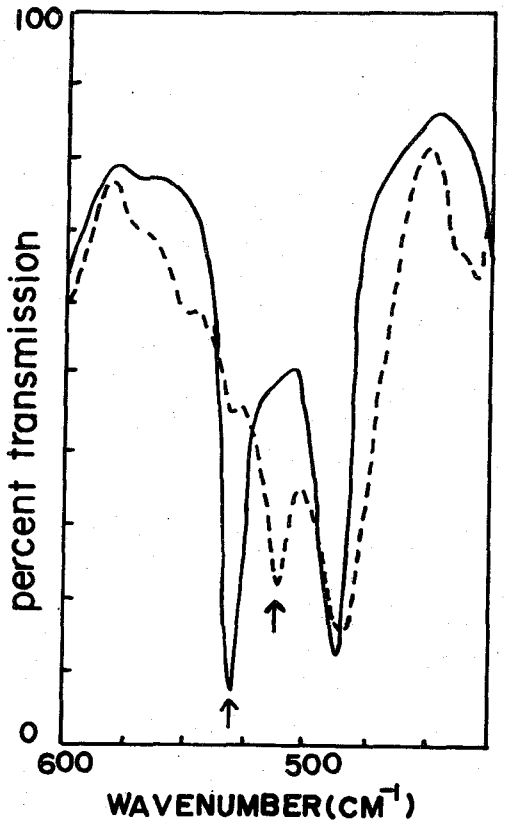

Fig. 2.3. Effect of annealing on infrared spectrum.
———, original specimen (form II (SGC))
------, specimen annealed for 20 hr at 185.8°C.

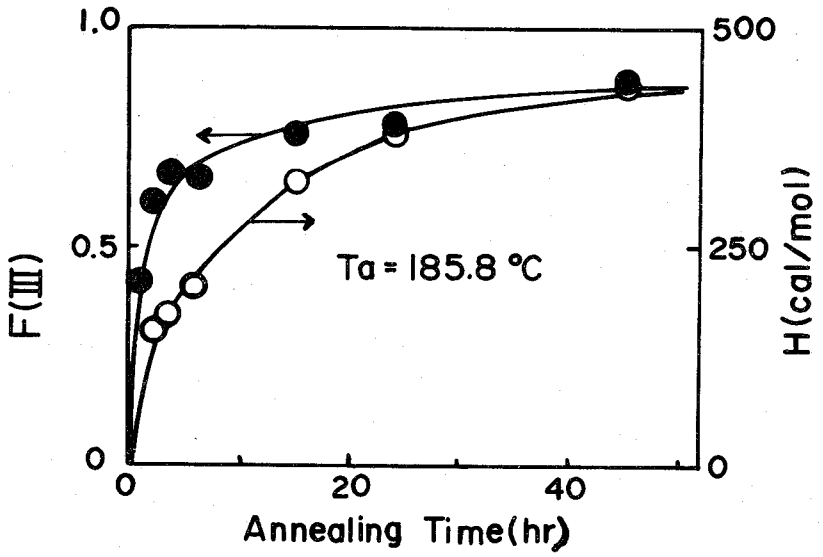

Fig. 2.4. Effects of annealing time on F(III) and endothermic enthalpy for form II (SGC) specimens at 185.8°C.

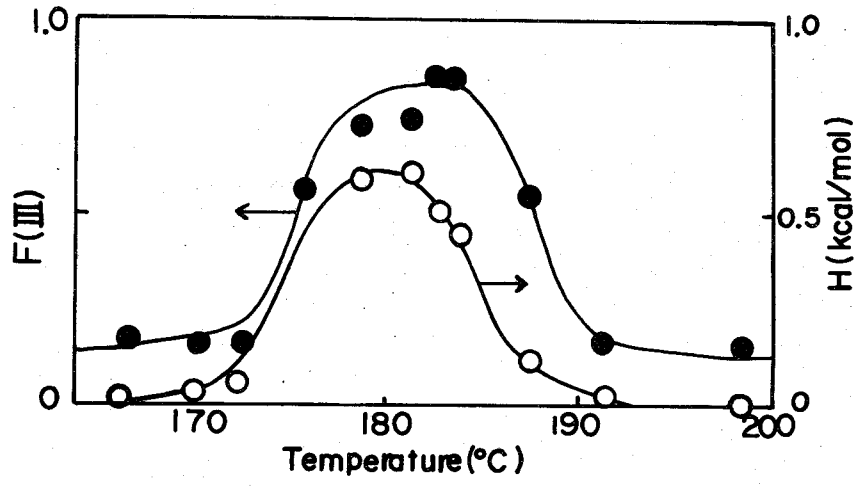

Fig. 2.5. Effects of temperature on F(III) and endothermic enthalpy for form II (SGC) specimens in the case of 20 hr annealing.

Figure 2.6a shows the DSC thermogram for unannealed form II (SGC), which displays only one peak at 174°C. On the other hand, according to Figure 2.6b, which shows the DSC thermogram for a form II (SGC) specimen annealed at 185.8°C for 20 hr, we see that another endothermic peak (199°C) appears above the annealing temperature T_a. Form II (SGC) specimens annealed for different periods of time at 185.8°C were subjected to DSC measurements,

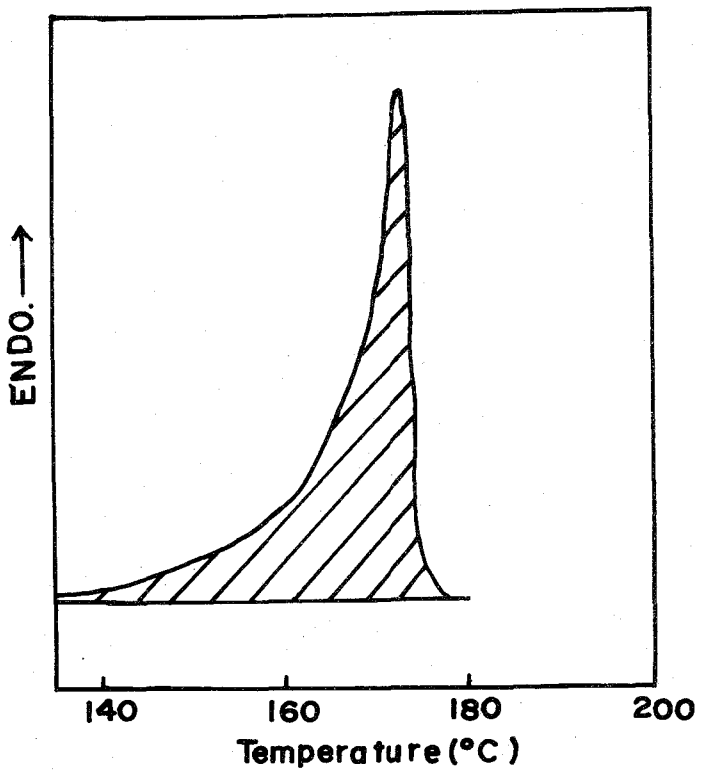

Fig. 2.6a. DSC thermogram of an unannealed form II (SGC) specimen.

which in all cases gave similar two peak thermograms. The enthalpy determined from the area under the higher temperature peak is plotted against the time of annealing in Figure 2.4; the curve rises with time in the same fashion as does F(III). Figure 2.5 shows that, for the annealing time of 20 hr, the endothermic enthalpy related to the higher temperature peak first increases and then decreases with raising temperature. This change in enthalpy is quite similar to that in F(III).

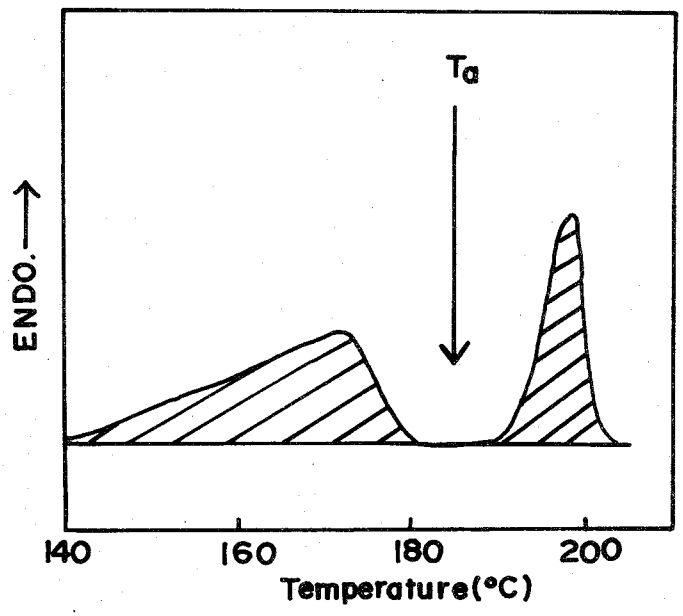

Fig. 2.6b. DSC thermogram for a form II (SGC) specimen annealed at T_a = 185.8°C for 20 hr.

These results suggest that the higher temperature peak may be associated with the fusion of form III crystals. In order to ascertain this point, we studied the temperature dependence of infrared spectra and X-ray patterns for the specimen prepared by annealing a form II (SGC) at 185°C for 20 hr. Figure 2.7 shows that the bands characteristic of forms II and III appear in the region from 700 to 900 cm^{-1} at room temperature. While the bands characteristic of form II (767, 796, 840, and 855 cm^{-1}) are absent above 180°C, those characteristic of form III (778, 809, and 833 cm^{-1})[14] are visible even at 183°C, and disappear only above 205°C. X-ray measurements on the same specimen at room temperature revealed reflections from both crystal forms II and III. The (110) reflection due to form II disappeared at about 185°C, whereas the (110) and (200) reflections due to form III persisted up to 210°C. Therefore, we conclude that the endothermic peak of the DSC curve at 199°C arises from the fusion of form III crystals.

As mentioned in the experimental section, F(III) determined from infrared spectra at room temperature probably includes a contribution from crystals that are formed during the cooling from the annealing temperature. However, the enthalpy associated with the higher temperature peak does not include such a contribution.

Nevertheless, as Figure 2.5 shows, the temperature dependence of F(III) is very similar to that of enthalpy, with some difference which may be noted in the region above 180°C. Therefore, F(III) was not appreciably affected by cooling.

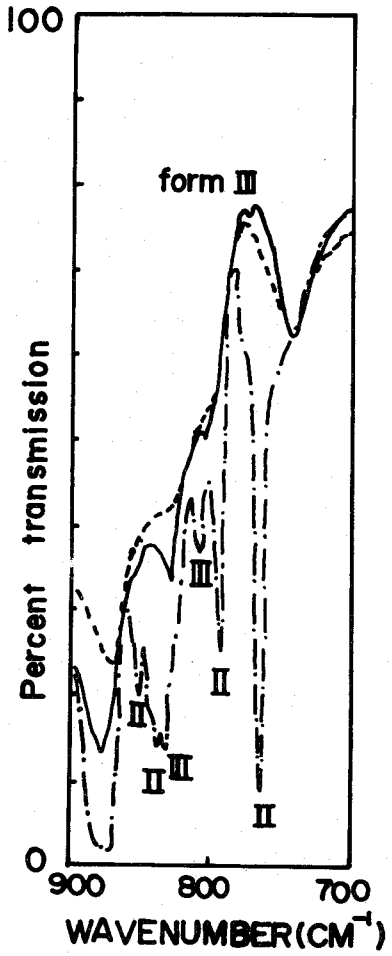

Fig. 2.7. Effects of temperature on the infrared spectrum of a PVDF specimen annealed at 185°C for 20 hr.

— - — - — : 25°C

——————— : 183°C

---------- : 205°C

2-3-2. Isothermal Crystallization of Molten Films

A PVDF film sandwiched between two pieces of thin teflon films (10μ) was placed between metal plates and melted above 210°C in a hot press. After having been cooled down to room temperature, the assembly composed of the PVDF film, teflon films, and metal plates was placed in a vessel under nitrogen atmosphere and heated again above 210°C to eliminate the thermal history of the specimen. Then crystallization from the molten PVDF was allowed to proceed isothermally at various fixed temperatures T_c, and after that the specimen was cooled to room temperature. Since the teflon films were easily separated from the PVDF film, adhesion of PVDF onto metal plates was thus obviated.

Figure 2.8 shows far-infrared spectra of the specimens isothermally crystallized at 161 and 170°C. Absorption bands characteristic of form III (300 cm^{-1} and 85 cm^{-1})[15] can be seen only in the specimen crystallized at 170°C. From the d-spacing of an X-ray diffraction pattern of the same specimen (see Figure 2.9), the predominant crystalline form was shown to be form III. Consequently we may conclude that form III can be obtained by isothermal crystallization at 170°C. It can be seen from Figure 2.9 that the crystallites of form III thus prepared are not oriented. Form III was also obtained when a PVDF film was sandwiched directly between metal plates and treated in the same way.

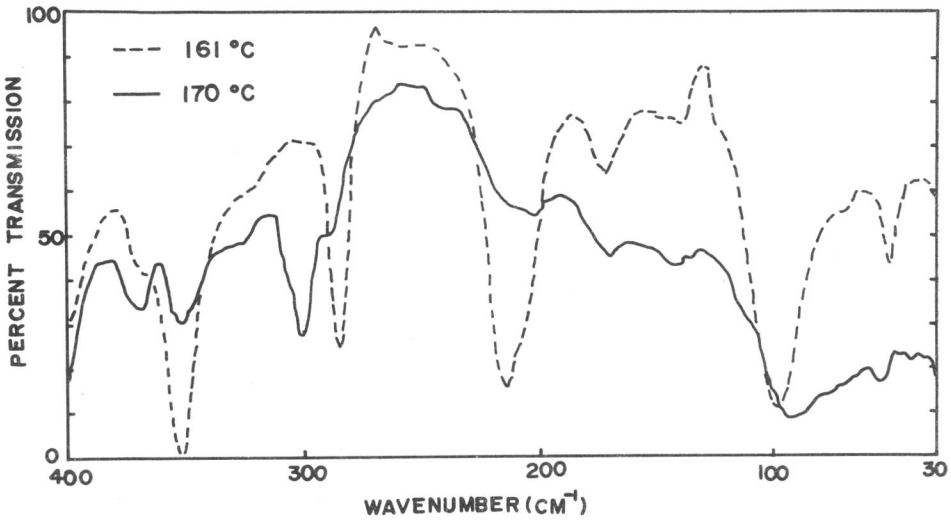

Fig. 2.8. Far-infrared spectra at room temperature of specimens crystallized at 161°C (------) and 170°C (———) for 20 hr from melt.

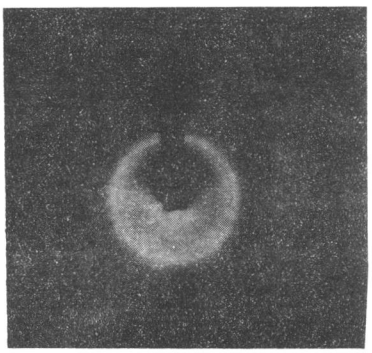

Fig. 2.9. X-ray diffraction pattern for a specimen crystallized at 170°C for 20 hr.

To explore further conditions favoring the formation of form III effects of crystallization temperature and time were studied by IR and DSC measurements. For a specimen crystallized at 166°C, F(III) determined by IR measurements are plotted against crystallization time in Figure 2.10. F(III) approaches an asymptotic value in about 20 hr. In Figure 2.11, F(III) after crystallization for 20 hr is plotted against crystallization temperature. It can be seen that the fraction of form III reaches a maximum between 165 and 175°C.

DSC thermograms of specimens crystallized isothermally between 165 and 170°C displayed three peaks. A typical example is illustrated in Figure 2.12. We denote these peaks by P_1, P_2, and P_3 in the order of decreasing temperature. Crystallizations at other temperatures gave only one or two of these peaks, as shown below.

The peak temperatures T_m for 20 hr crystallization are plotted against crystallization temperature T_c in Figure 2.13. It can be seen that all the three peaks shift to higher temperatures with raising T_c. The T_m for the P_2 peak is higher than 165°C and it is the only peak produced by crystallization above 170°C. The T_m for the P_3 peak is lower than 170°C. Though not indicated here, only the P_3 peak was observed below 155°C.

Figure 2.14a shows plots of the enthalpies associated with the three peak against T_c. The plots for the P_1 and P_2 peaks exhibit maxima at about 155 and 170°C, respectively, whereas that for the P_3 peak displays an abrupt rise below 165°C. Below 155°C, only the P_3 peak was observed.

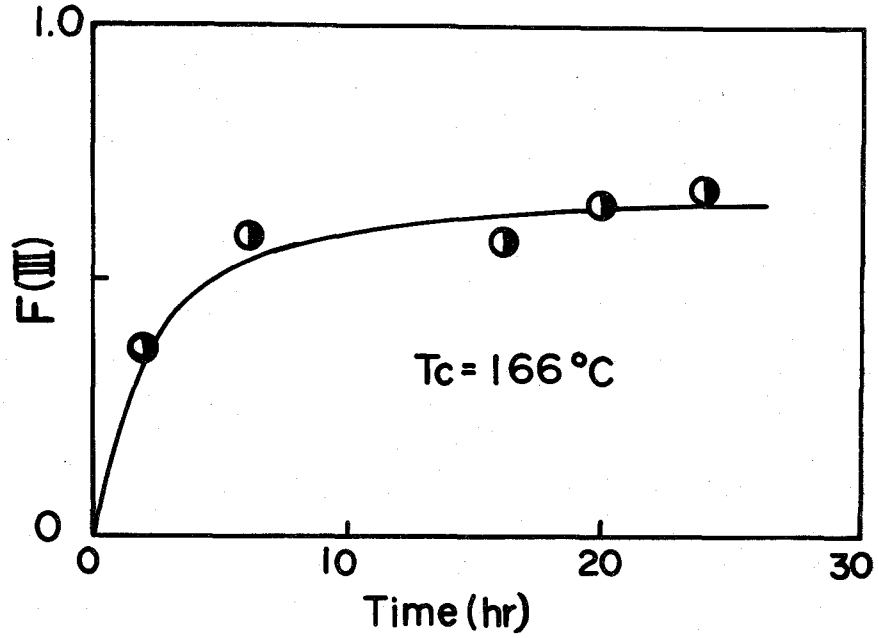

Fig. 2.10. Time dependence of F(III) in isothermal crystallization of melt at 166 °C.

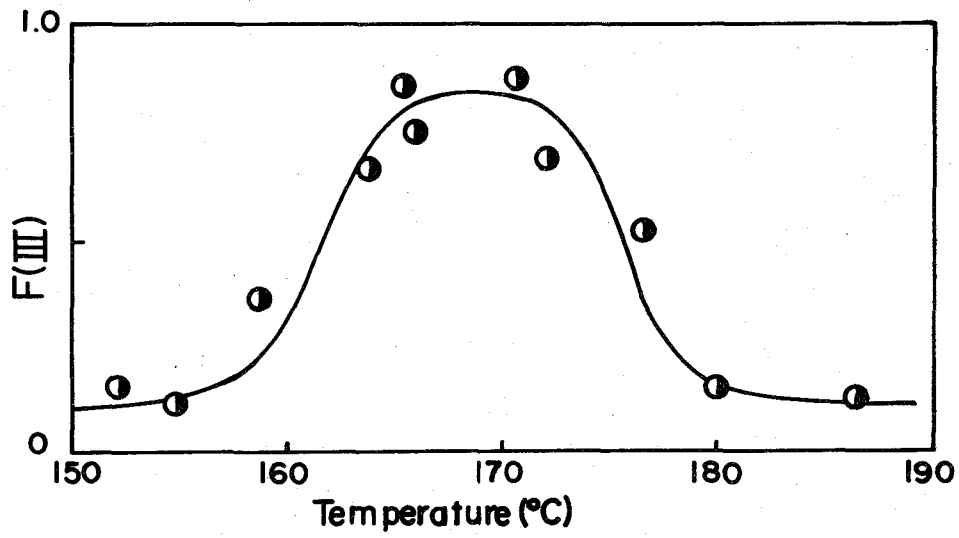

Fig. 2.11. F(III) of specimens crystallized for 20 hr at different temperatures from melt.

By studying specimens which showed only one or two peaks on the DSC thermogram, we tried to assign the peaks to appropriate crystal forms. Specimens crystallized below 160°C showed only one peak and the peak temperature followed the P_3 line in Figure 2.13. These specimens gave X-ray patterns and IR spectra characteristic of form II. Hence, the P_3 peak was considered to be attributable to the fusion of form II crystals.

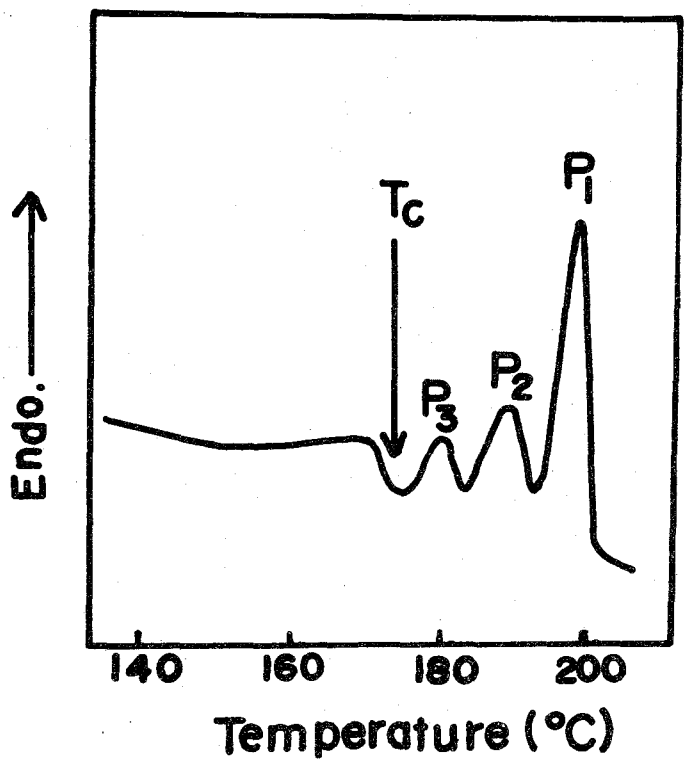

Fig. 2.12. DSC thermogram of a specimen isothermally crystallized at T_c = 169°C for 20 hr: P_1, high temperature peak; P_2, intermediate temperature peak; P_3, low temperature peak.

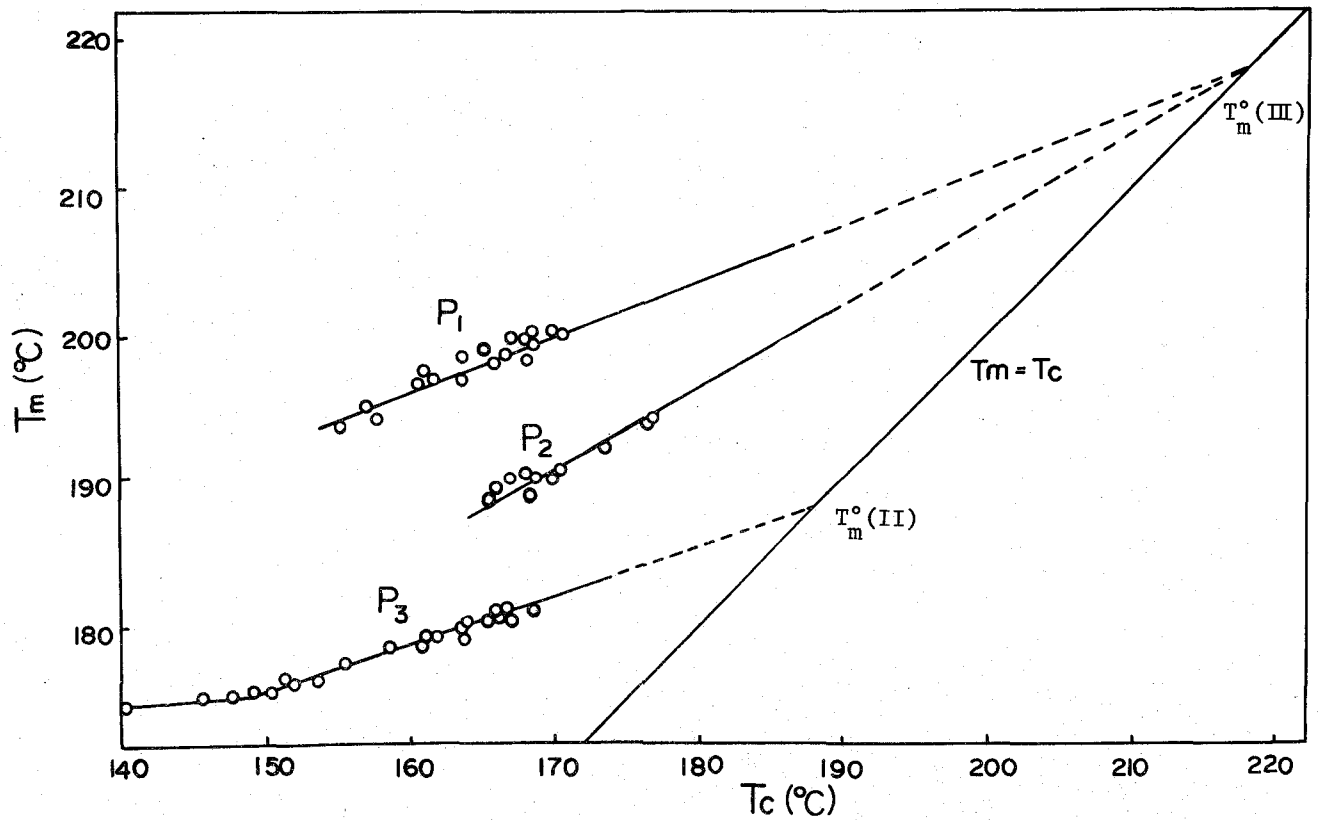

Fig. 2.13. Peak temperature T_m vs. crystallization temperature T_c: T_m°, equilibrium melting temperature; P_1, high temperature peak; P_2, intermediate temperature peak; P_3, low temperature peak.

A specimen crystallized at 164°C for 20 hr gave two peaks on the DSC thermogram (Figure 2.15). The higher temperature peak conforms to the P_1 line in Figure 2.13 and the lower temperature one to the P_3 line. The X-ray photograph of the sample indicated that forms II and III coexisted at room temperature. The infrared spectra (Figure 2.16) also showed the presence of these crystalline forms at room temperature and at 165°C. At 185°C, bands characteristic of form II diminished, whereas those characteristic of form III remained visible. At 205°C, the band indicating form III vanished. In order to illustrate these changes, absorbances at 767 cm^{-1} (form II) and 778 cm^{-1} (form III) are plotted against temperature in Figure 2.17. Here, the data have been corrected for radiation from the specimen at elevated temperatures. As shown in Figure 2.17, the absorbance at 767 cm^{-1} becomes zero above 180°C, while the absorbance at 778 cm^{-1} persists to about 205°C. At the temperatures between 180 and 205°C, only the absorbance at 778 cm^{-1} (form III) can be observed. These results are consistent with the conclusion that the P_1 peak is associated with the fusion of form III.

Figure 2.13 shows the peak temperatures T_m plotted against the crystallization temperatures T_c. At about 218°C, two extrapolated lines of the P_1 and P_2 peaks for form III intersect the straight line of $T_m = T_c$. Extrapolation of the data for the P_3 peak for form II gives the temperature of the intersection of about 188°C. From the points of intersection the equilibrium melting temperatures are estimated to be about 218°C for form III and about 188°C for form II. The P_2 peak appears always at temperatures higher than the equilibrium melting temperature for the form II crystal. This fact also suggests that the P_2 peak is not due to

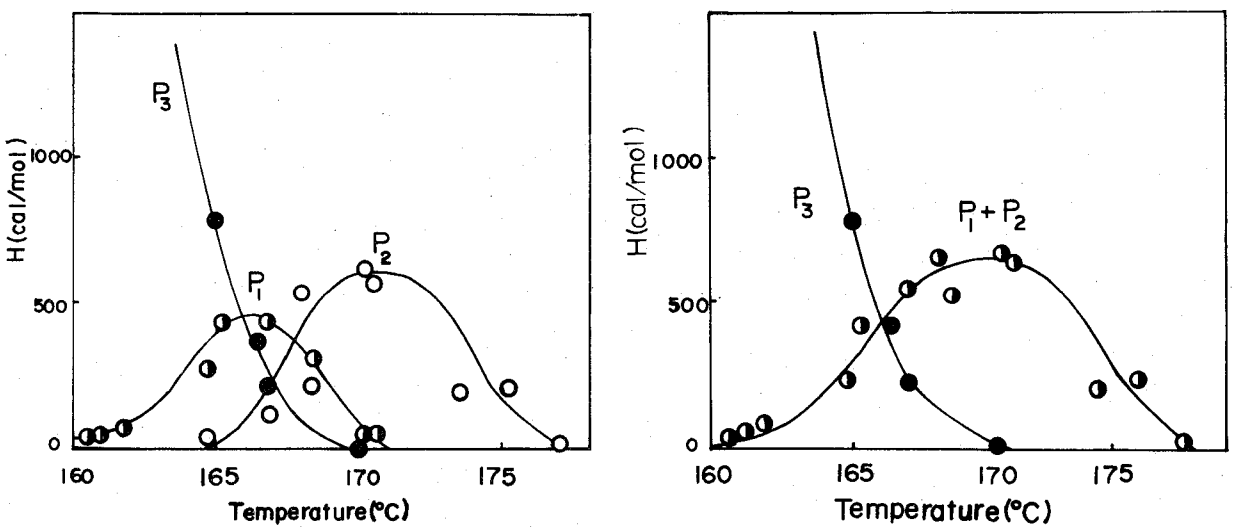

Fig. 2.14. Endothermic enthalpies associated with the peaks in DSC thermograms of specimens crystallized for 20 hr at various fixed temperatures. P_1, high temperature peak; P_2, intermediate temperature peak; P_3, low temperature peak.

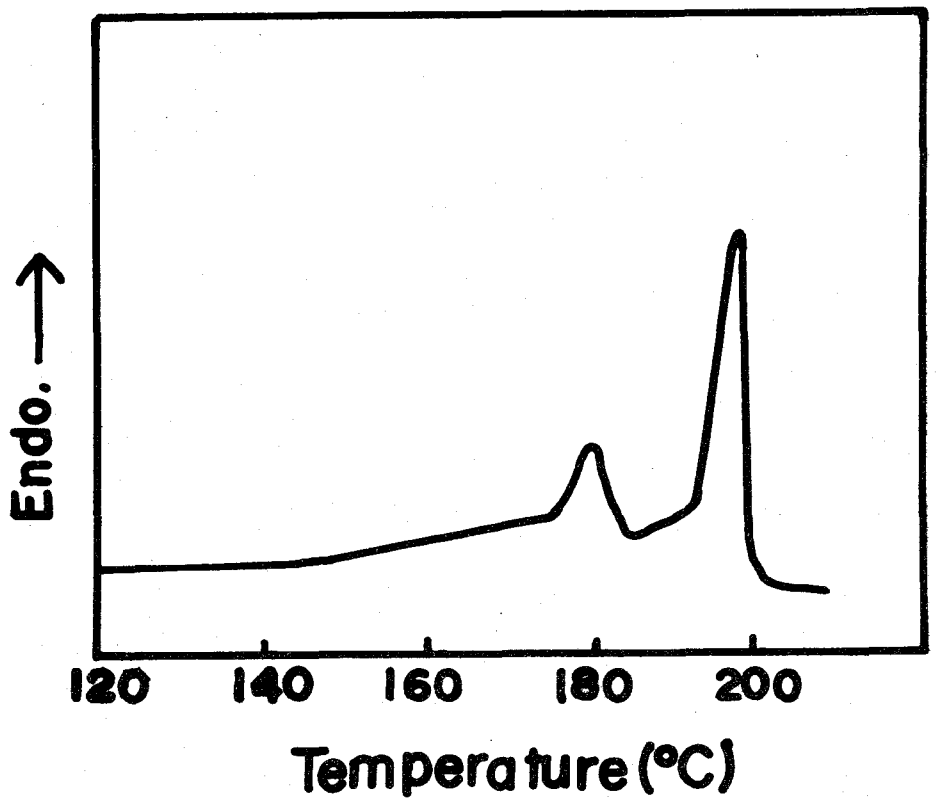

Fig. 2.15. DSC thermogram of a specimen crystallized for 20 hr at 164°C.

the fusion of form II. By isothermal crystallization near 170°C, we obtained specimens giving a DSC curve in which peaks other than the P_2 peak were barely detectable: see Figure 2.14a. The IR spectrum and X-ray photograph of such a specimen indicated that it was in form III. These findings further support the idea of ascribing the P_2 peak to the fusion of form III. If the enthalpy value for each peak is regarded as a measure of the amount of the respective crystalline form, the sum of the enthalpies for P_1 and P_2 should be proportional to the total amount of form III.

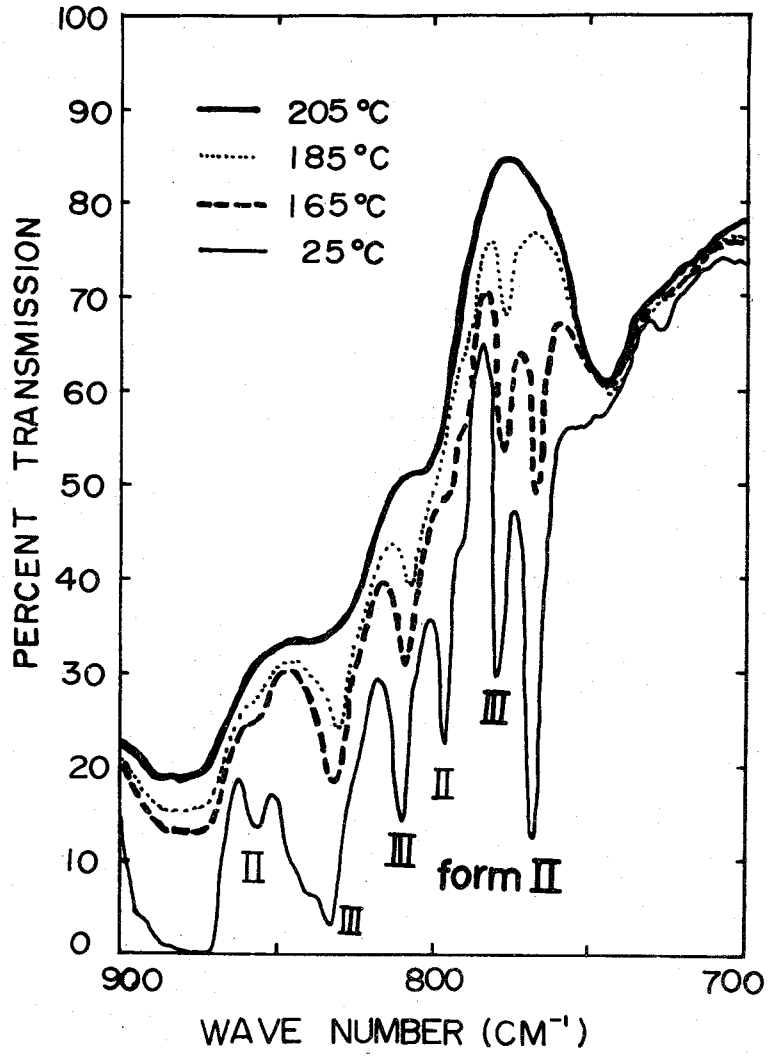

Fig. 2.16. Temperature dependence of infrared spectrum of a specimen crystallized for 20 hr at 164°C.

Figure 2.14b shows plots of the values for the sum against crystallization temperature T_c, which exhibits a broad maximum around 170°C. Thus we may conclude that the growth of form III crystallites from the melt is favored in the range between 160 and 180°C, while that of form II is favored below 160°C. Figure 2.14b suggests that the optimum crystallization temperature for form III is higher than that for form II. The results were not appreciably altered by the extension of crystallization time up to one week. Hence, the rapid decrease in the fraction of form III may be independent of crystallization time.

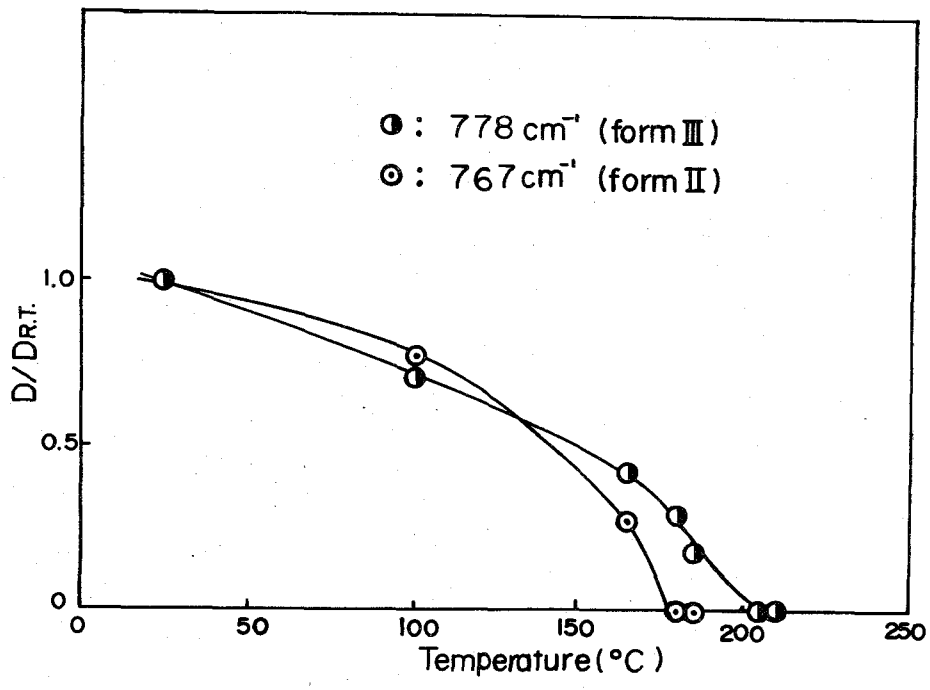

Fig. 2.17. Temperature dependence of absorbances D at 767 cm^{-1} (form II) and 778 cm^{-1} (form III). $D_{R.T.}$ denotes absorbance at room temperature.

Figure 2.14 indicates that the growth of form II crystals is favored as the temperature is lowered below 165°C. Thus quenching to room temperature will accelerate the formation of form II , while crystallization at near 170°C will favor only the formation of form III. When the sample crystallized isothermally is cooled to room temperature, both form II and form III crystals must develop. However, in the lower temperature region, the growth of form III crystal was so slow that the infrared measurements on a specimen quenched from the melt showed only a trace amount of form III.

Finally, let us compare Figures 2.5 and 2.11 to discuss the optimum conditions for the formation of form III crystal by isothermal crystallization and annealing. The maximum in Figure 2.11 occurs near 170°C, while that in Figure 2.5 appears near 180°C. A possible explanation for this difference of optimum temperatures is that in the case of annealing, nuclei of form II crystals may remain during annealing even at 170°C, so that the development of form III is hindered. In isothermal crystallization from the melt, on the other hand, crystallization starts after melting, and hence the growth of form III crystals may proceed without hindrance by remaining crystallites.

References

1. Yu. D. Kondrashov, Trudy Gosudarst. Inst. Priklad. Khim., 166 (1960).
2. N. I. Makarevich and V. N. Nikitin, Vysokomol. Soed., 7, 1673 (1965).
3. K. Okuda, T. Yoshida, M. Sugita, and M. Asahina, J. Polym. Sci., B, 5, 465 (1967).
4. Ye. L. Gal'perin and B. P. Kosmynin, Vysokomol. Soed., 11, 1432 (1967).
5. G. Natta, G. Allegra, I. W. Bassi, D. Sianesi, G. Gaporiccio, and E. Torti, J. Polym. Sci., A, 3, 4263 (1965).
6. J. B. Lando, H. G. Olf, and A. Peterlin, J. Polym. Sci., A-1, 4, 941 (1966).
7. W. W. Doll and J. B. Lando, J. Macromol. Sci., B2, 219 (1968).
8. G. Cortili and G. Zerbi, Spectrochim. Acta., 32A, 2216 (1967).
9. R. Hasegawa, M. Kobayashi, and H. Tadokoro, Polymer J., 3, 591 (1972).
10. K. Nakagawa and Y. Ishida, J. Polym. Sci., A-2, 11, 2153 (1973).
11. Ye. L. Gal'perin, B. P. Kosmynin, and V. K. Smirnov, Vysokomol. Soed., 8, 1880 (1970).
12. J. D. Hoffman and J. J. Weeks, J. Res. Nat. Bur. Stand., 66A, 13 (1962).
13. S. Enomoto, Y. Kawai, and M. Sugita, J. Polym. Sci., A-2, 6, 861 (1968).
14. M. Kobayashi, K. Tashiro, and H. Tadokoro, private communication.
15. M. Kabayashi, K. Tashiro, and H. Tadokoro, The abstract of 30th Annual Meeting of Japan Chemical Society, p. 159 (1974).

Chapter 3

Anomalously Dielectric Dispersion of Form II Poly(vinylidene Fluoride) in the Low Frequency Region

3-1. Introduction

The low frequency dielectric behavior of form II PVDF at high temperatures is apt to superimpose on another process which gives rise to anomalously large values of ε' and ε''. It has been presumed that this process may arise from ionic impurities contained in the sample.[1,2] This chapter is concerned with a verification of such presumption. The idea here is that if ionic impurities are responsible for the process concerned, there should be obtained a drastic reduction in ε' and ε'' at low frequencies and high temperatures by subjecting the sample to a static electric field of appropriate strength before dielectric measurement. Furthermore, one may inject additional ions into the sample by application of such field. Then one should observe an enhanced anomaly in dielectric dispersion in the region of low frequencies. The experiments described in the present chapter were designed so as to check these predictions.

3-2. Experimental

Throughout the study in this chapter we used form II (MQ) specimens for measurements.

Figure 3.1 shows schematically the assembly that was used to inject ions into sample films. A 1-mm thick disk of LiCl, NaCl, or $CaCl_2$ made by pressing the powder under 200 kg/cm^2 was sandwiched between a pair of

sample films. Two layers of aluminum foil were inserted between each of the films and the electrode that faced it.

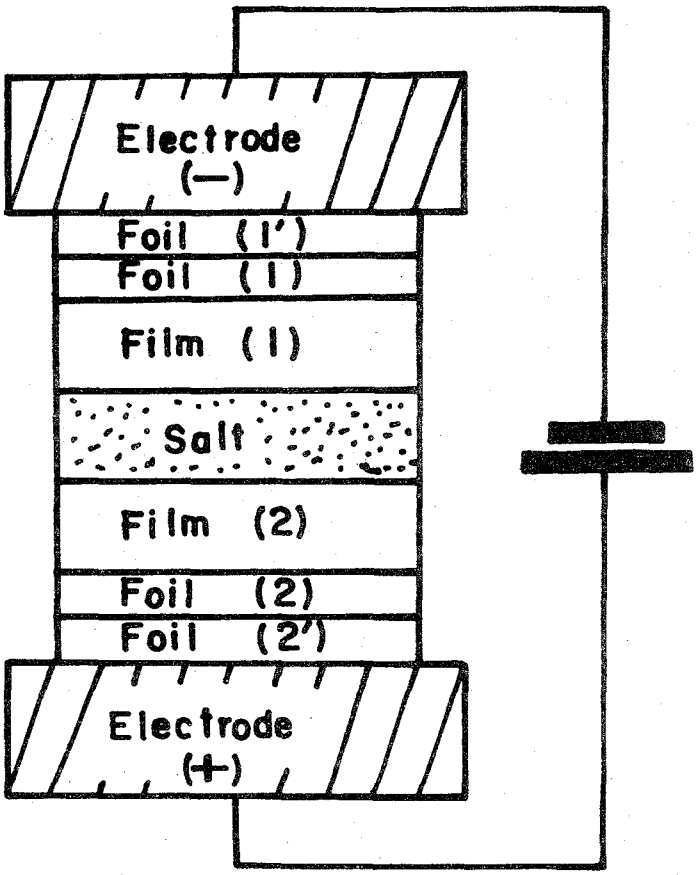

Fig. 3.1. Schematic diagram of assembly for injecting ions into polymer films: Films (1) and (2), form II (MQ) PVDF films; Foils (1), (1'), (2) and (2'); aluminum foils.

A dc electric field of 10 KV/cm was applied between the pair of electrodes at 160°C for an interval of 120 hr, and then the inserted aluminum foils 1 and 2 were analyzed by emission spectroscopy. The characteristic wavelengths used for identification were 3232.61 and 4603.00 Å for lithium, 3302.323 Å for sodium, and 3933.666 and 3968.468 Å for calcium. The spectrum of Fe was used for establishing the wavelength. As a reference material for the cations use was made of $LiCO_3$ for lithium, NaCl for sodium, and $CaCl_2$ for calcium. Carbon electrodes were used for the spark.

Before carrying out dielectric measurements the sample films were annealed at 160°C for 24 hr in order to disperse the injected ions uniformly. A reference specimen was prepared by treating a fresh film under a dc electric field of 10 KV/cm at 160°C for 120 hr, followed by annealing at 160°C for 24 hr.

The aluminum foils 1' and 2' were used to protect the inner foils 1 and 2 from contamination arising from the brass electrodes. These foils were 0.02 mm thick. The salt disks were dried under vacuum at room temperature before insertion into the assembly. The entire assembly was placed in an air-tight vessel, which in turn was evacuated and flushed with dry nitrogen.

3-3. Resutls and Discussion

3-3-1. Effect of Static Electric Field

Figures 3.2 and 3.3 illustrate the frequency dependence of ε' and ε'' for a fresh specimen of form II (MQ) at various temperatures. It is

seen that both ε' and ε'' at higher temperatures undergo a sharp upturn as the frequency is lowered. The corresponding data for the same specimen exposed to a static electric field of 25 KV/cm at 160°C for 24 hr before dielectric measurements are shown in Figures 3.4 and 3.5. One observes that the anomalous rises in ε' and ε'' at low frequencies are virtually absent in these graphs. These changes must have been caused primarily by the removal of ionic impurities which would have been contained in

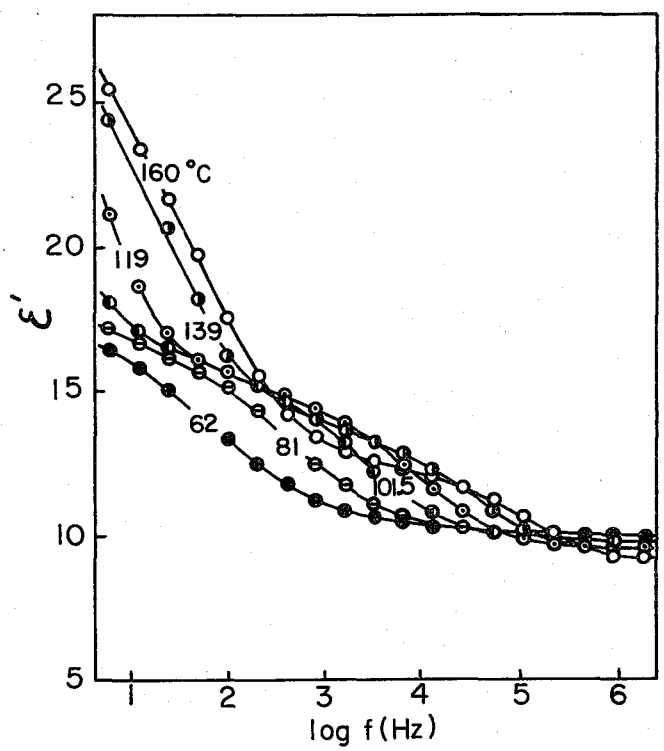

Fig. 3.2. Frequency dependence of ε' at various fixed temperatures for a form II (MQ) specimen.

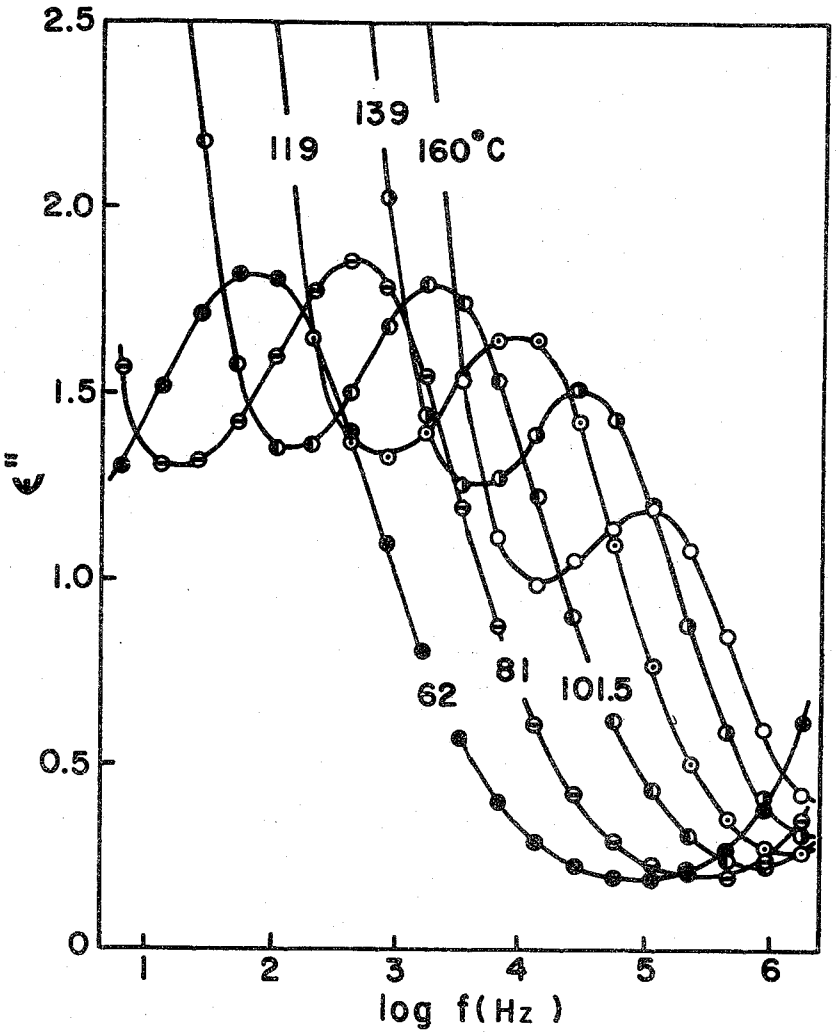

Fig. 3.3. Frequency dependence of ε'' at various fixed temperatures for a form II(MQ) specimen

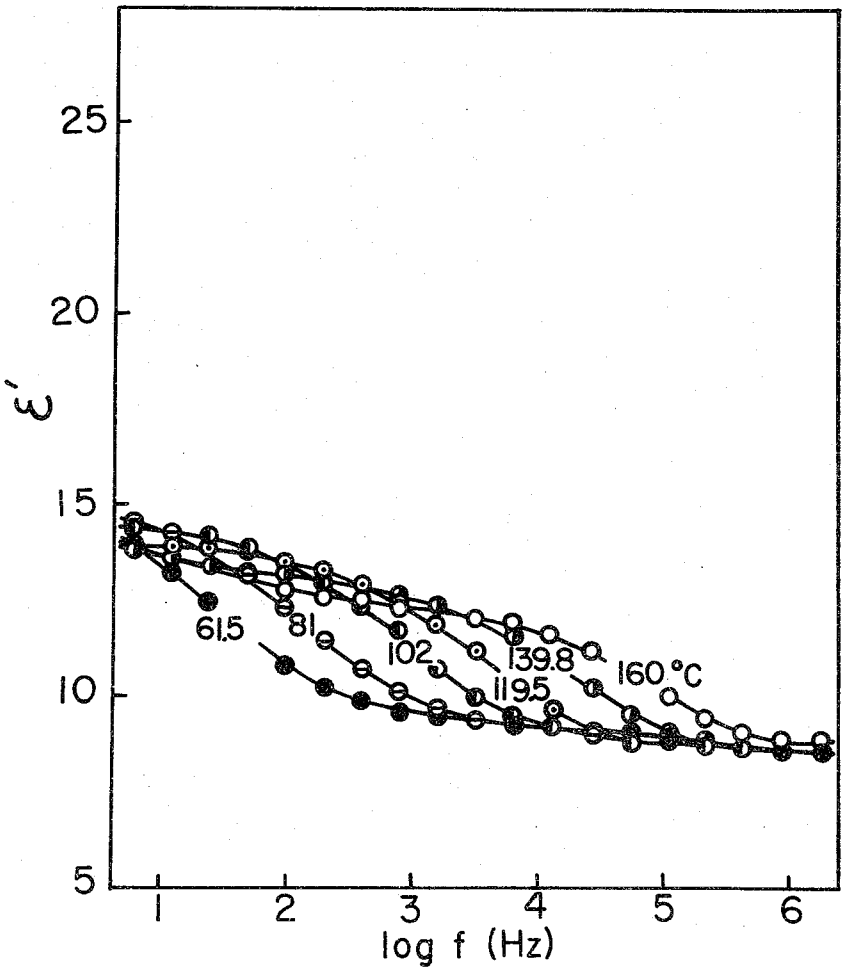

Fig. 3.4. Frequency dependence of ε' at various fixed temperatures for a form II (MQ) specimen to which a field of 25 KV/cm was applied at 160 °C for 24 hr.

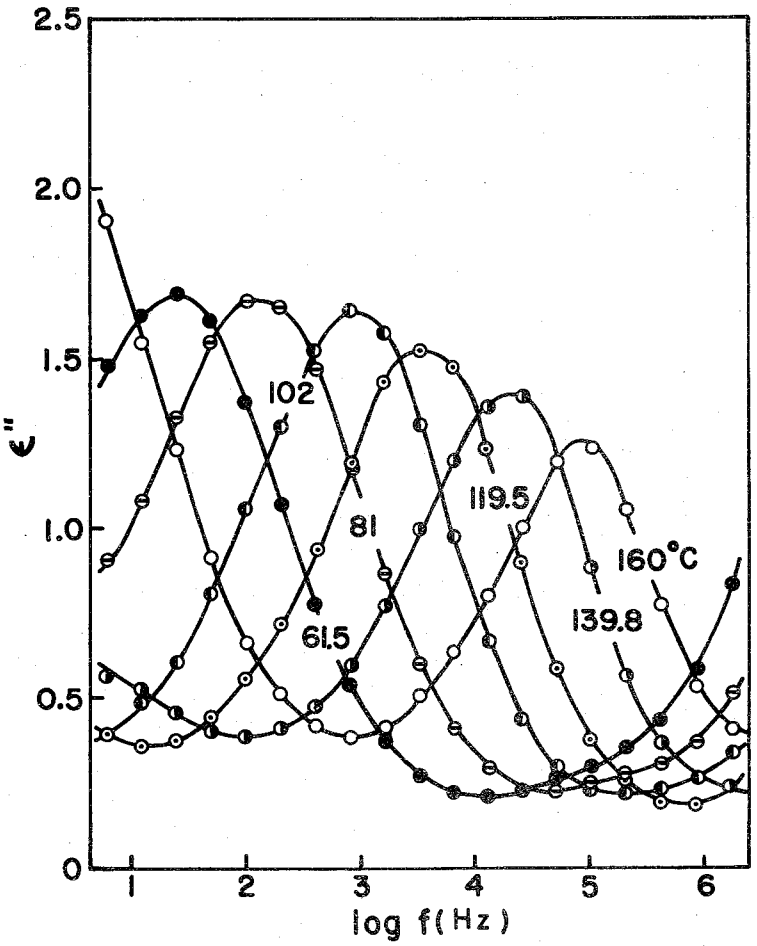

Fig. 3.5. Frequency dependence of ε'' at various fixed temperatures for a form II (MQ) specimen to which a field of 25 KV/cm was applied at 160 °C for 24 hr.

the fresh specimen. However, the effect of annealing, which took place during the application of a static electric field, may not be ignored, because generally the dielectric properties of crystalline polymers undergo changes upon annealing. The data shown in Figures 3.6 and 3.7 indicate that annealing of a fresh form II (MQ) sample for 24 hr had

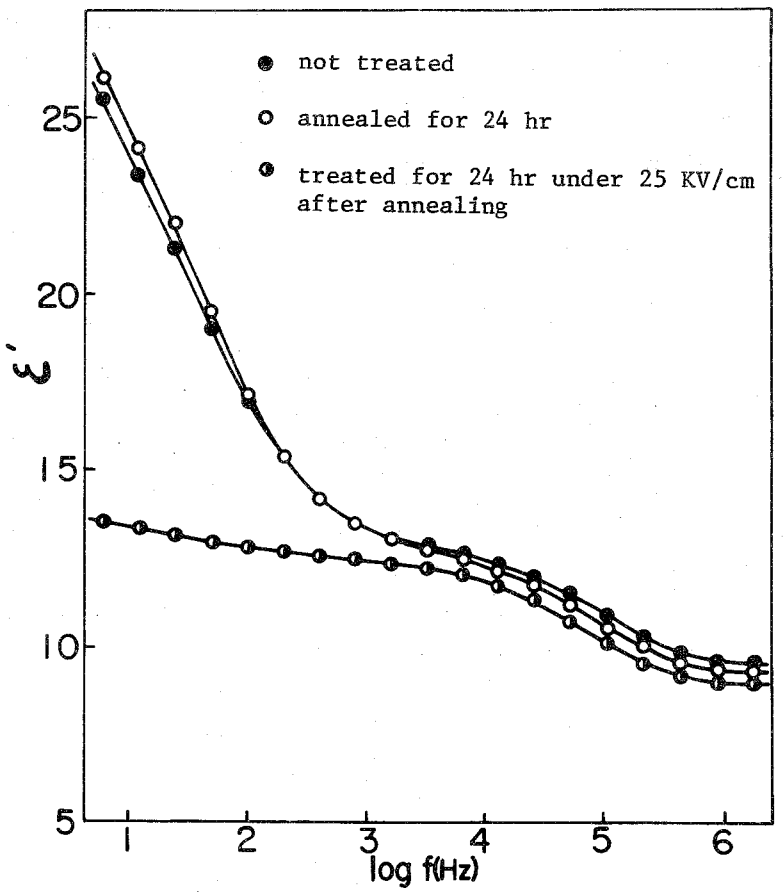

Fig. 3.6. Effects of annealing and static electric field on ε' of a form II (MQ) specimen at 160°C.

virtually no effect on both ε' and ε'' at 160°C and that application of a static electric field had a decisive influence.

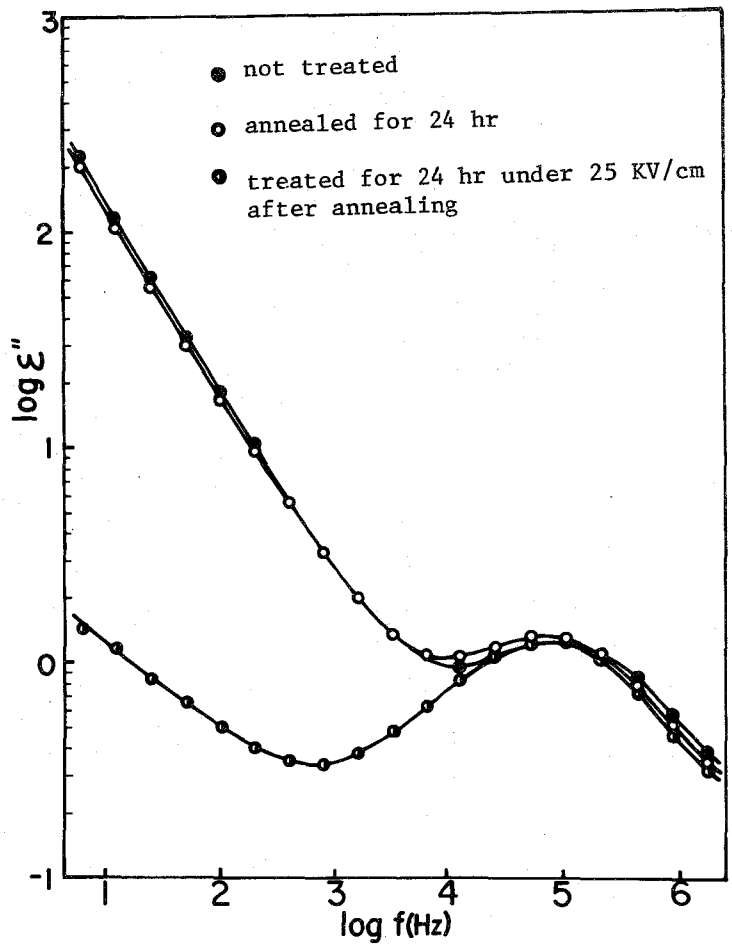

Fig. 3.7. Effects of annealing and static electric field on ε'' of a form II (MQ) specimen at 160°C.

The field effect is more appreciable at lower frequencies. The trend can be clearly demonstrated by plotting the decrease in ε'', $\Delta\varepsilon''$, caused by application of 25 KV/cm for 24 hr at 160°C against frequency; see Figure 3.8. The plotted points in the figure follow accurately the equation

$$\log \Delta\varepsilon'' = A - B \log f \qquad (3\text{-}1)$$

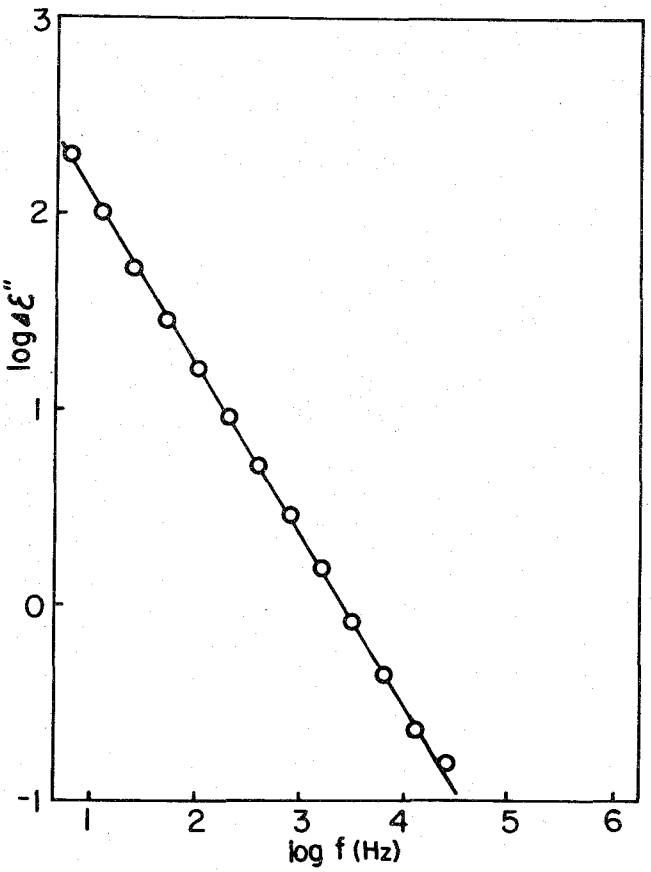

Fig. 3.8. $\Delta\varepsilon''$ caused by application of 25 KV/cm to a form II (MQ) specimen for 24 hr at 160°C plotted against log of frequency.

where A and B are constants. It was found that B was approximately equal to unity and independent of the temperature of dielectric measurement.

The decrease in ε'' during the application of a static electric field is shown for three field strengths in Figure 3.9. As expected, there occurs a more rapid decrease in ε'' as the field strength becomes larger.

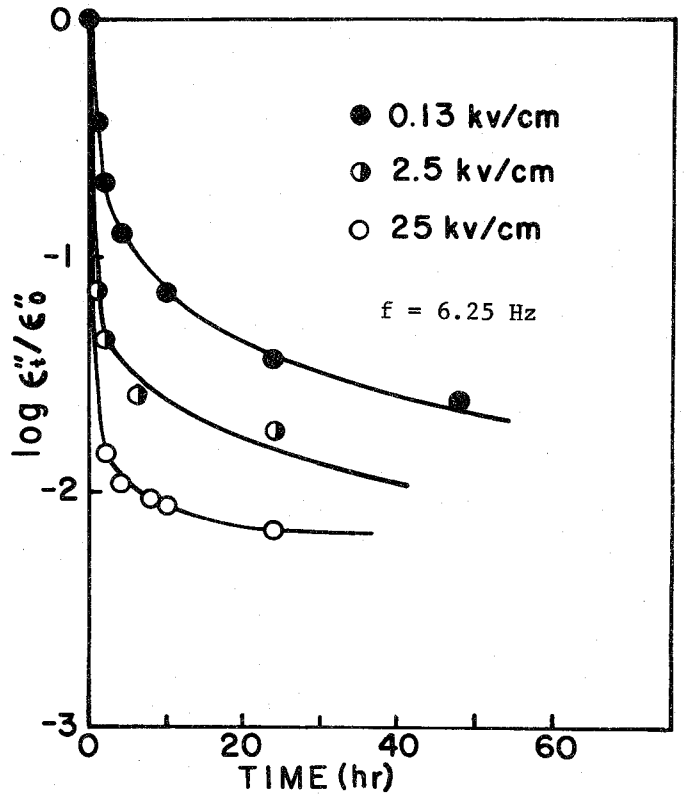

Fig. 3.9. Field strength dependence of the decrease of ε'' with time at 160°C: ε''_o, initial value; ε''_t, value at time t.

Figure 3.10 and 3.11 show what happened in ε' and ε'' when the applied field was removed after the sample had been subjected to a static

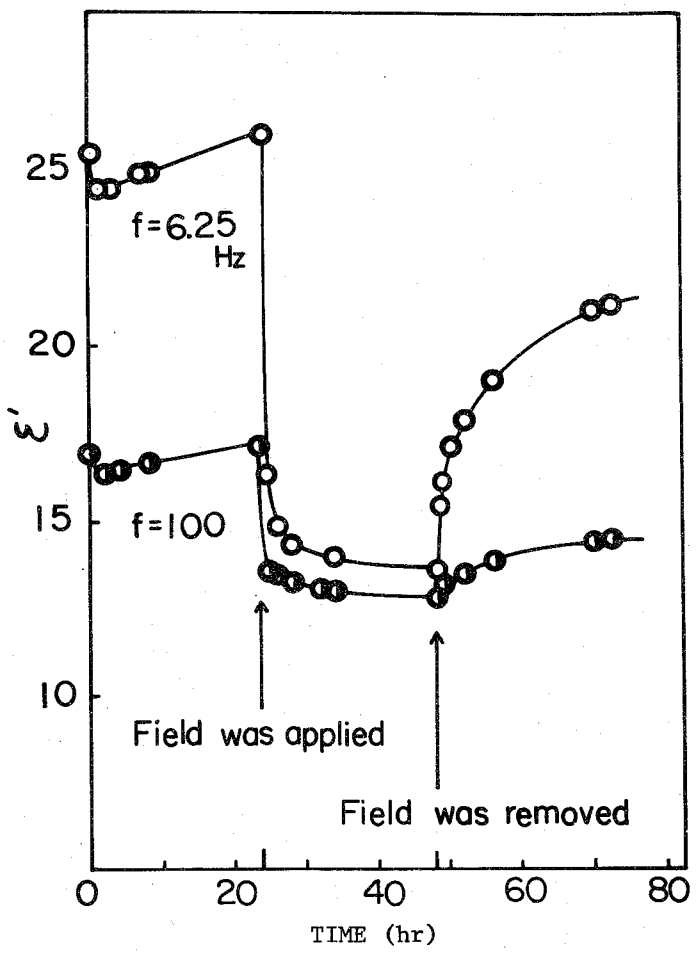

Fig. 3.10. Change of ε' with time. After a form II (MQ) specimen had been annealed at 160°C for 24 hr, a field of 25 KV/cm was applied for 24 hr at 160°C and then removed.

electric field for a fixed period of time. The time variations of ε' and ε'' shown in these figures can be interpreted in terms of the migration of ionic impurities.

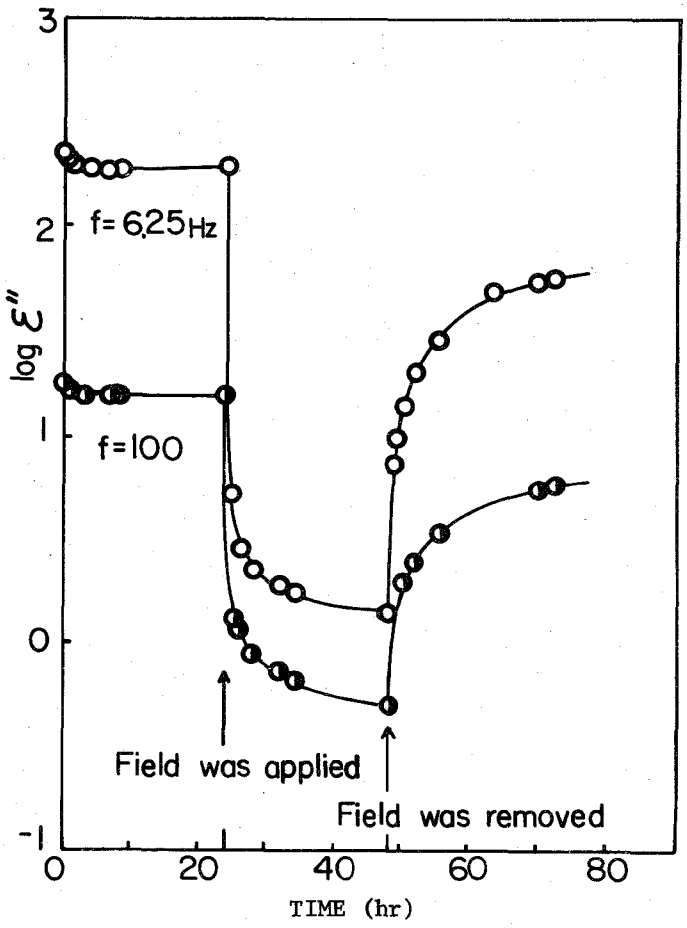

Fig. 3.11. Change of ε'' with time. After a form II (MQ) specimen had been annealed at 160°C for 24 hr, a field of 25 KV/cm was applied for 24 hr at 160°C and then removed.

Ions initially distributed uniformly in the specimen are forced to displace toward the electrodes and are concentrated during the application of a static electric field. The concentration of ions results in a reduction of their mobilities, which, in turn, should bring about a decrease in the complex dielectric constant. The decrease cannot occur instantaneously, because the migration of ions experiences viscous resistance from the surrounding polymer matrix. When the applied field is removed, the concentrated ions tend to diffuse by thermal agitation back to the original uniform distribution. This change should cause an increase in the complex dielectric constant, at a rate primarily dependent on the rate of diffusion of ions. These considerations explain the major features of the experimental data in Figures 3.10 and 3.11. It is to be noted that the ultimate recovery of ε' and ε'' is incomplete. Electrolysis of ionic impurities may account for this effect.

According to Kakutani,[3] trace amounts of ions such as Na, Ca, S, and Cl are contained in commercial PVDF films. This information substantiates the considerations described above. In order to remove the silver electrodes in the dielectric measurement cell without scratching the specimen we made an amalgam by rolling a small droplet of mercury on its surface. When this amalgam was analyzed by emission spectroscopy, the presence of calcium was detected, but no other impurities were identified.

If, as argued above, the anomalous increases in ε' and ε'' at low frequencies are caused by ionic impurities, the extent of their suppression by static electric field should depend strongly on the temperature of measurement, since migration of ions requires appropriate free

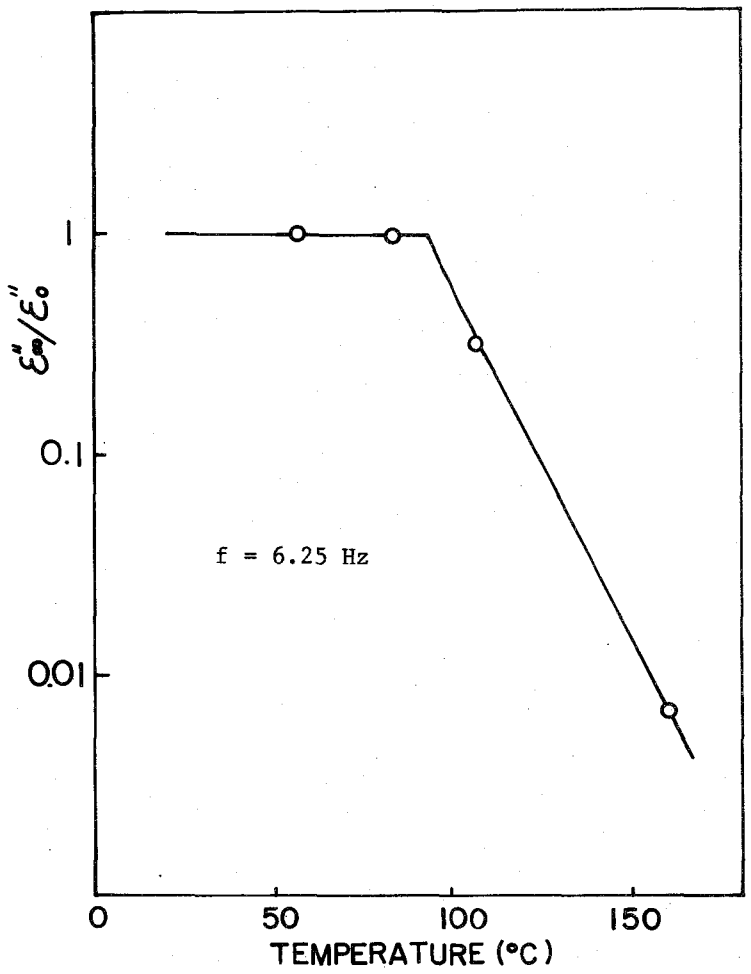

Fig. 3.12. Decrease of ε'' caused by a static electric field against the temperature of measurement. The ratio $\varepsilon''_\infty/\varepsilon''_o$ is used to represent the decrease of ε'' . ε''_∞, asymptotic value; ε''_o, initial value; frequency, 6.25 Hz; field strength, 25 KV/cm.

volumes which depend on temperature. The experimental data shown in Figure 3.12 indicate that this prediction is valid at temperatures above about 90°C. Below this temperature the local viscosity may be too high or the free volume is too small for ions to migrate in the PVDF solid.

3-3-2. Injection of Metal Ions

The results of emission spectroscopy for the foils 1 and 2 are presented in Figure 3.13. The characteristic lines at 3232.61 and 4603.00 Å for lithium can be seen in the spectra for $LiCO_3$ and the foil 1. However, they are absent in the spectra for the foil 2, the reference foil, and carbon, as seen from Figure 3.13a. Thus we find that lithium ions deposited on the foil 1. In Figure 3.13b, the characteristic line at 3302.323 Å for sodium is observed in the spectra for the foil 1 and NaCl, but not in the spectra for the foil 2 and carbon. Thus sodium ions also deposited on the foil 1. Figure 3.13c indicates that the characteristic lines at 3933.666 and 3968.468 Å for calcium are observable in the spectra for the foil 1 and $CaCl_2$, but not in the spectra for the foil 2 and carbon. This means that calcium ions also deposited on the foil 1.

No anionic species could be detected on the foil 2 because of the difficulties in the analytical technique. We failed to observe the characteristic lines at 4819.46, 4810.06, 4794.54 Å for chlorine even with a halide.

The deposition of lithium, sodium, and calcium on the foil 1 evidenced that these negative ions were injected and migrated through the PVDF film by the application of a static electric field. This fact substantiates the idea of interpreting the aforementioned effects of

applied electric field on the dielectric constant and loss in terms of the induced migration of ionic impurities contained in the specimen. Because now it is possible to inject an additional quantity of ions into the sample film by a static electric field, one should be able to observe even more appreciable rises of ε' and ε'' at low frequencies than is possible with the fresh film. The prediction is confirmed by the

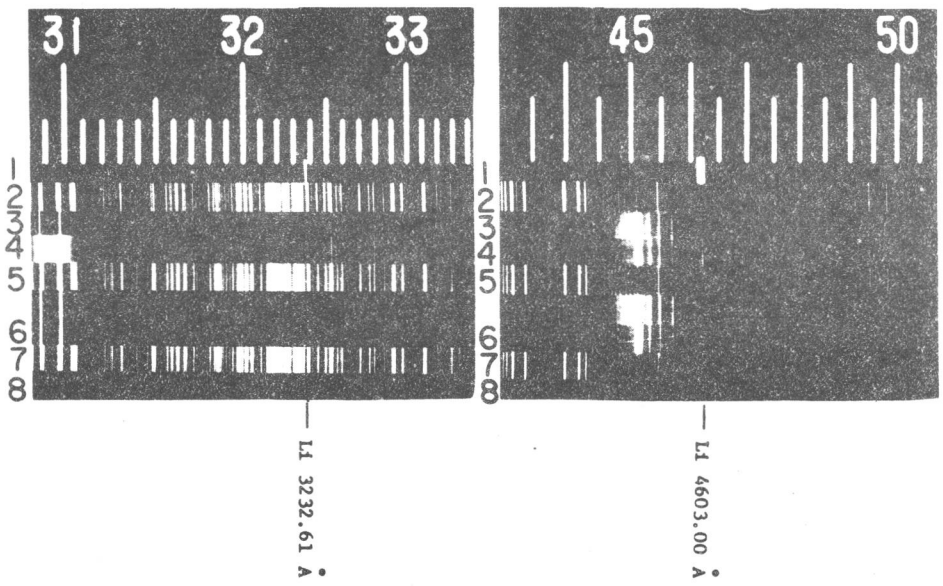

Fig. 3.13a. Emission spectra for a form II (MQ) specimen, to which a dc electric field of 10 KV/cm was applied at 160°C for 120 hr; 1. $LiCO_3$; 2. Fe; 3. foil 2; 4. foil 1; 5. Fe; 6. foil (reference); 7. Fe; 8. carbon.

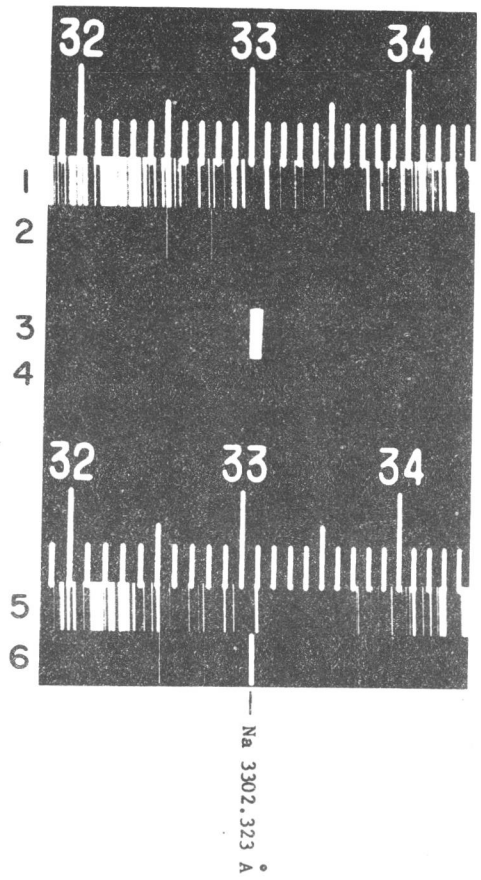

Fig. 3.13b. Emission spectra for a form II (MQ) specimen, to which a dc electric field of 10 KV/cm was applied at 160 °C for 120 hr: 1. Fe; 2. foil 2; 3. NaCl; 4. carbon; 5. Fe; 6. foil 1.

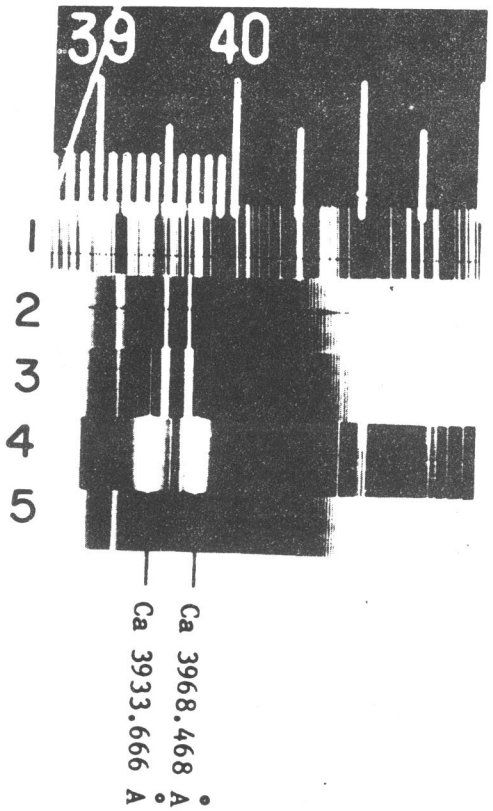

Fig. 3.13c. Emission spectra for a form II (MQ) specimen, to which a dc electric field of 10 KV/cm was applied at 160 °C for 120 hr: 1. Fe; 2. foil 2; 3. foil 1; 4. $CaCl_2$; 5. carbon.

data on the film 1 in Figure 3.14, which refer to the injection of Na^+ from a NaCl disc. Though not shown here, the corresponding data for ε' exhibited a similar feature, and also the injection of Li^+ and Ca^{++}

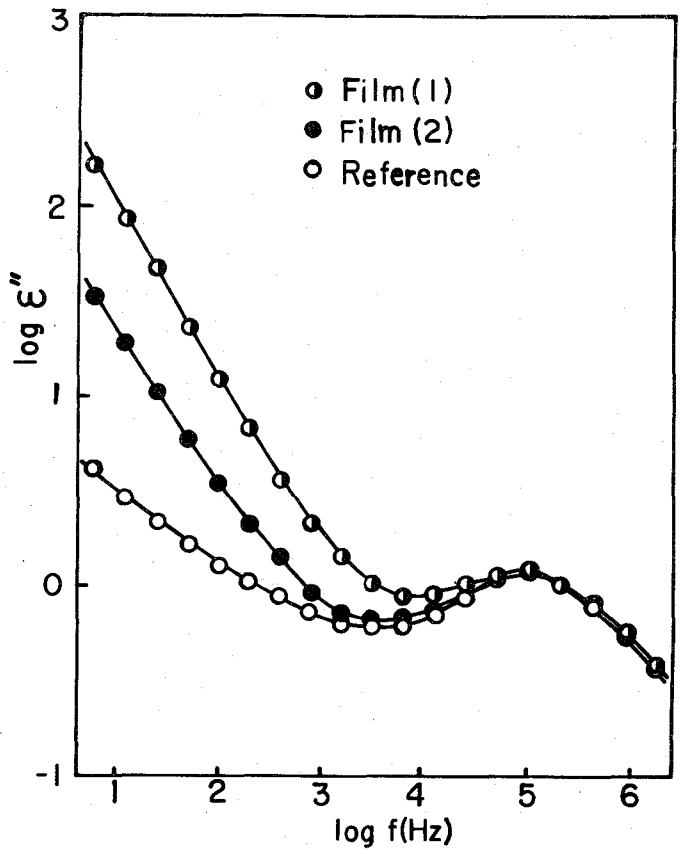

Fig. 3.14. Effects of ions injected from NaCl disc upon frequency dependence of ε'' at 160°C for a form II (MQ) specimen. The notation of Film (1) and Film (2) refers to Fig. 3.1. Film (1): Na^+ ions injected; Film (2): Cl^- ions injected.

gave similar results. Note that a certain fraction of injected ions passes through the film, deposites on the electrode, and thus does not contribute to dielectric behavior.

When, for example, a NaCl disc is used for injection, Cl^- ions should be injected into the film 2, although, as mentioned above, we failed to detect directly those which migrated through the film and deposited on the foil 2. The data on the film 2 in Figure 3.14 provide indirect evidence for this expectation. The sharp upturn of ε'' for this film at low frequencies must have been caused by Cl^- ions injected from the NaCl disc. The difference from the curve for the film 1 may be attributed primarily to a smaller mobility of Cl^- ions than Na^+ ions.[4]

References

1. Y. Ishida, O. Amano, and M. Takayanagi, Kolloid-Z., 172, 129 (1960).
2. Y. Ishida, M. Watanabe, and K. Yamafuji, Kolloid-Z., 200, 48 (1964).
3. H. Kakutani, private communication.
4. C. Turbandt, H. Reinhold, and G. Liebold, Z. Anorg. Allegem. Chem., 197, 225 (1931).

Chapter 4

High Temperature Dielectric Relaxation of Form II Poly(vinylidene Fluoride)

4-1. Introduction

Dielectric dispersion studies so far carried out on crystalline PVDF have exclusively concerned themselves with samples of form II. There are opposite opinions about the origion of the high temperature relaxations observed with such samples.[1-7] Peterlin and Holbrook,[1] Boyer,[2] Paul and Altamirano,[3] and Ciu[4] have expressed the opinion that this type of relaxation arises from molecular motions in the amorphous region of the polymer. On the other hand, Sasabe et al.[5] and Yano[6] have argued that it is attributable to the crystalline region of the polymer. Nakagawa and Ishida[7] have presented data which were in favor of the opinion of the latter authors. In this chapter, we present more confirmative evidence for the fact that the high temperature dielectric relaxation of form II PVDF is associated with molecular motions in the crystalline region.

4-2. Experimental

Measurements were made with form II (MQ) and form II (SGC) PVDF specimens prepared as described in Chapter 2, together with melt-quenched Kynar specimens. The last ones were obtained by moulding purified powder of Kynar between metal plates at 180°C and quenching the melt film into water. X-ray and IR measurements indicated that the crystallites in a Kynar film thus obtained was 1.758 g/cm^3 at 25°C. In what follows, the Kynar specimens are referred to as form II (Kynar).

4-3. Results and Discussion

Figure 4.1 shows the temperature dependence of ε'' at 100 Hz for a form II (MQ) sample. The sharp rise of ε'' at temperatures above about 120°C is due to ionic impurities contained in the sample. In fact, it could be eliminated by application of a static electric field before dielectric measurement, as the data for form II (MQ) in Figure 4.2 illustrate.

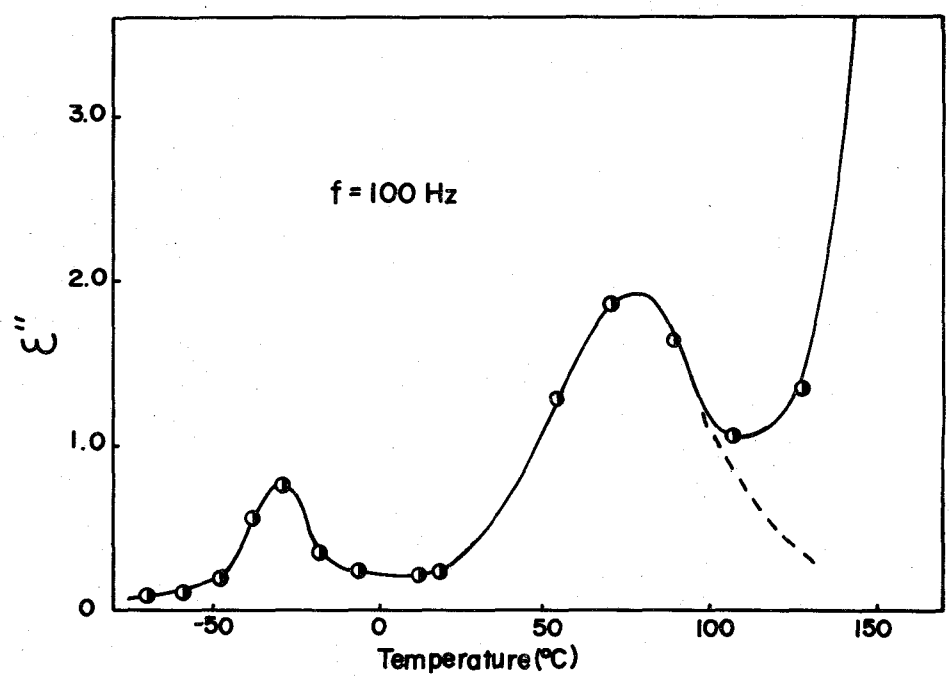

Fig. 4.1. Temperature dependence of ε'' at 100 Hz for a form II (MQ) specimen. The dotted line represents the values obtained by applying a static electric field of 30 KV/cm for 40 hr at 160°C.

Figure 4.2 also contains ε'' data at 100 Hz for form II (SGC) and form II (Kynar) specimens. It is seen that the high temperature relaxation appears more pronouncedly in form II (SGC) than in form II (MQ) and form II (Kynar), while the latter two specimens exhibit a marked relaxation in the temperature region between -50 and 0°C.

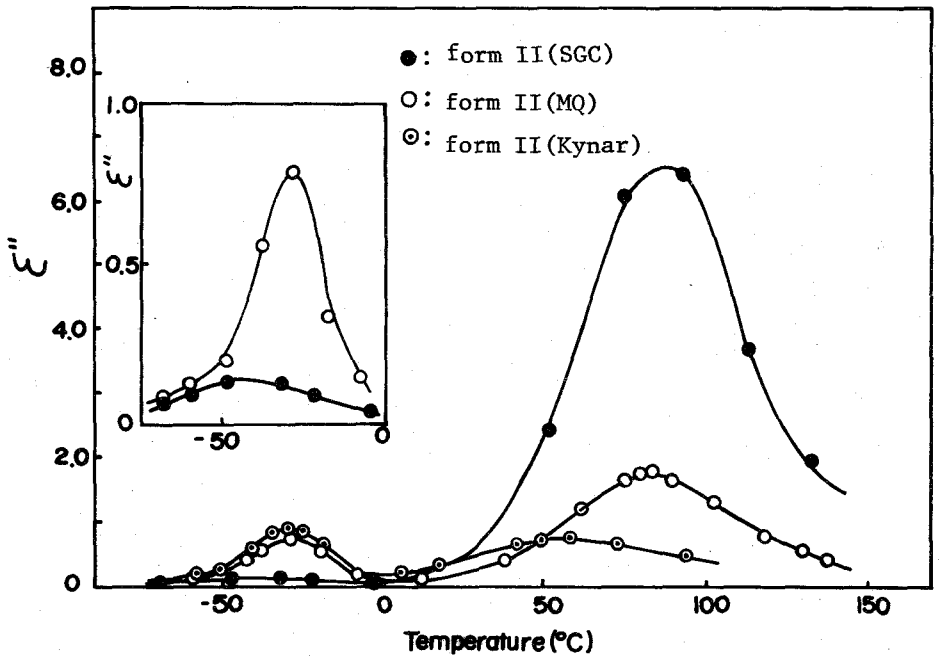

Fig. 4.2. Comparison of ε'' vs. temperature curves at 100 Hz for various specimens. The ionic contribution was suppressed by applying a static electric field.

However, it should be noted that, as the graph in the insert reveals, form II (SGC) exhibits another weak dispersion at about -50°C.

The densities and degrees of crystallinity of these three specimens were in the order: form II (SGC) > form II (MQ) > form II (Kynar). This fact, together with the relationship that the strengths of high temperature relaxation for the three specimens are also in the same order, suggests that the crystalline region of form II PVDF should be responsible for its high temperature dielectric dispersion. On the other hand, the intermediate temperature relaxation, i.e., the one that appeared in the range -50° to 0°C, may be a reflection of microbrownian motions in the amorphous region of the polymer.[5-7] For it appears more pronouncedly in a less crystalline specimen. Previous investigators[5-7] observed still another dielectric dispersion as a shoulder in the lower temperature trail of the intermediate temperature relaxation curve. The present measurement on form II (SGC) disclosed such low temperature relaxation as a distinct peak located at about -50°C. This consequence arose from the fact that the intermediate temperature relaxation of this specimen was almost entirely suppressed for its high degree of crystallinity.

If the high temperature relaxation of PVDF is associated with the crystalline region, it should disappear when the sample is melted. On the other hand, if it arises from molecular motions in the amorphous region, its strength should increase upon melting.[8] The validity of the former prediction can be claimed from the data shown in Figure 4.3, in which the frequency dependence of ε'' for form II (MQ) at various temperatures is shown. The temperature of 178°C is about 3°C above the

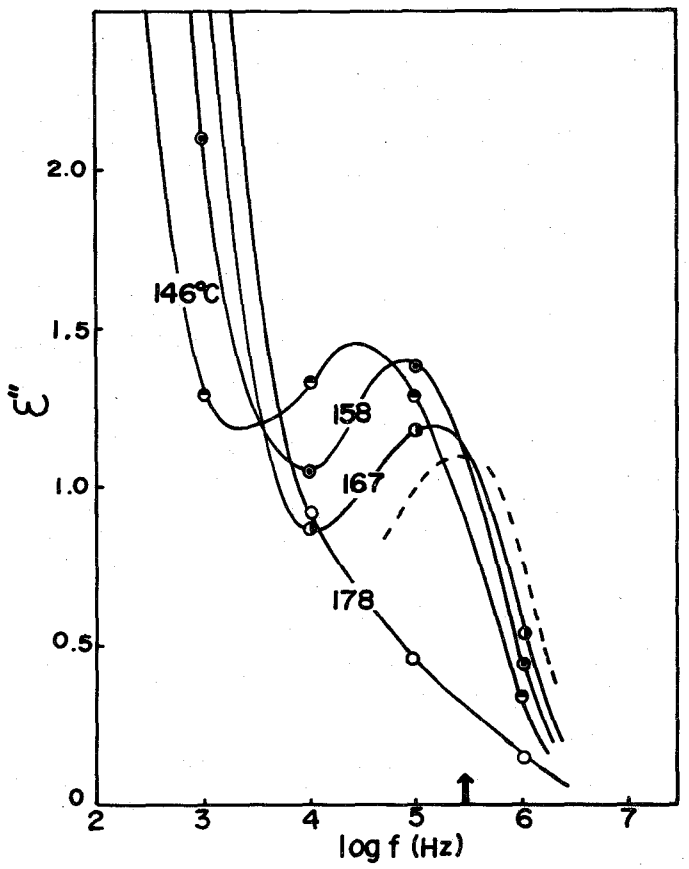

Fig. 4.3. Frequency dependence of ε'' at indicated temperatures for a form II (MQ) specimen. The dotted line represents ε'' vs. log f curve at 178°C drawn on the assumption that the shape of ε'' vs. log f curve not change and the peak value decreases with increasing temperature. The arrow indicates the location of the peak at 178°C extrapolated from Figure 4.5.

melting point of the sample and the crystallites are supposed to melt completely at this temperature, as can be understood from the DSC thermogram shown in Figure 4.4. The ε'' versus log f curve for this temperature in Figure 4.3 exhibits no peak, in contrast to the corresponding

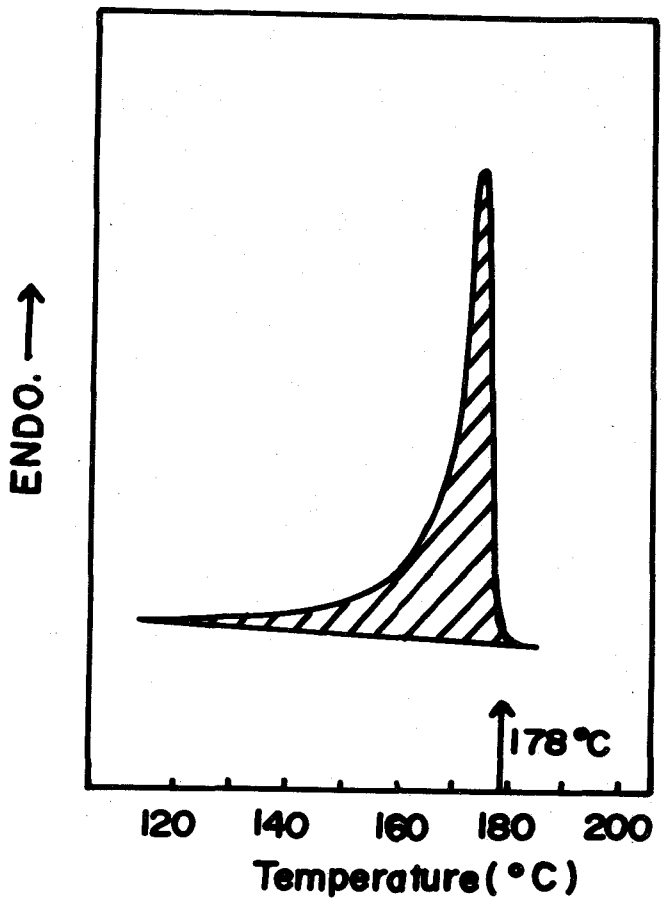

Fig. 4.4. DSC thermogram for a form II (MQ) specimen with a heating rate of 10°C/min.

curves for the lower temperatures. These facts allow us to conclude with confidence that the high temperature dielectric dispersion of PVDF ought to be an effect arising from the crystalline portions in the sample.

Figure 4.5 shows that the Arrhenius plot for the peak frequency f_m of the high temperature relaxation is linear. By extrapolation of the α_c plot the f_m at 178°C is estimated to be 300 KHz. If normalized with the maximum value of ε'' for each curve, the three curves but that for 178°C in Figure 4.3 can be superimposed on a single curve by appropriate

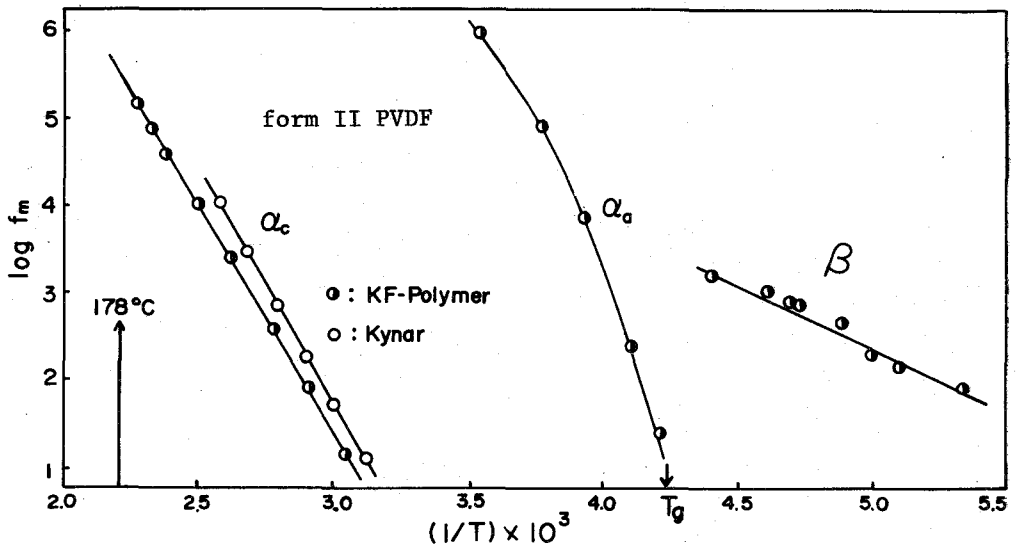

Fig. 4.5. Arrhenius plots for the three relaxation processes. In this map, the high temperature relaxation, the intermediate temperature relaxation, and the low temperature relaxation are called α_c, α_a, and β, respectively.

horizontal displacement. The dashed line in this figure represents the ε'' versus log f curve which would be obtained at 178°C from such a superimposed curve. As expected, its maximum appears at f = 300 KHz. The significant disparity between this predicted curve and the actual experimental data at 178°C implies that all crystallites in the sample virtually disappear at a temperature even only 3°C above the melting point.

References

1. A. Peterlin and J. D. Holbrook, Kolloid-Z., 203, 68 (1965).
2. R. F. Boyer, private communication.
3. D. R. Paul and J. O. Altamirano, Amer. Chem. Soc., Div. Polymer Chem., Reprints, 15 (1), 409 (1974).
4. Jen Ciu, private communication.
5. H. Sasabe, S. Saito, M. Asahina, and H. Kakutani, J. Polym. Sci. A-2, 7, 1405 (1969).
6. S. Yano, J. Polym. Sci. A-2, 8, 1057 (1970).
7. K. Nakagawa and Y. Ishida, J. Polym. Sci. A-2, 11, 1503 (1973).
8. R. H. Boyd and C. H. Porter, J. Polym. Sci., A-2, 10, 647 (1972).

Chapter 5

High Temperature Dielectric Relaxation of Form III Poly(vinylidene Fluoride)

5-1. Introduction

As described in Chapter 2, samples of form III PVDF dimensionally stable at high temperatures can be prepared by isothermal crystallization. This finding made it possible to study high temperature dielectric relaxation of form III PVDF. The present chapter described results from such a study.

5-2. Experimental

Samples of form III PVDF prepared by isothermal crystallization are here referred to as form III (ISO). Comparative data were taken with form II (MQ) specimens.

5-3. Results and Discussion

Figure 5.1 shows the temperature dependence of ε' and ε'' for form III (ISO) at various fixed frequencies. The steep rises both in ε' and ε'' with temperature are striking. Thus, at 100 Hz, ε' undergoes an almost tenfold increase when the temperature is raised from 150°C toward the melting point of the sample (198°C). The sharp drop in ε' beyond the melting point is even more striking; above 200°C the values of ε' almost diminish to zero. Also at 100 Hz, ε'' reaches a very sharp maximum at about 180°C, and rises again at temperatures above 200°C after passing through a narrow minimum. The maxima in ε'' shift to high temperatures as the frequency is increased. The sharp rise in ε'' sbove 200°C is

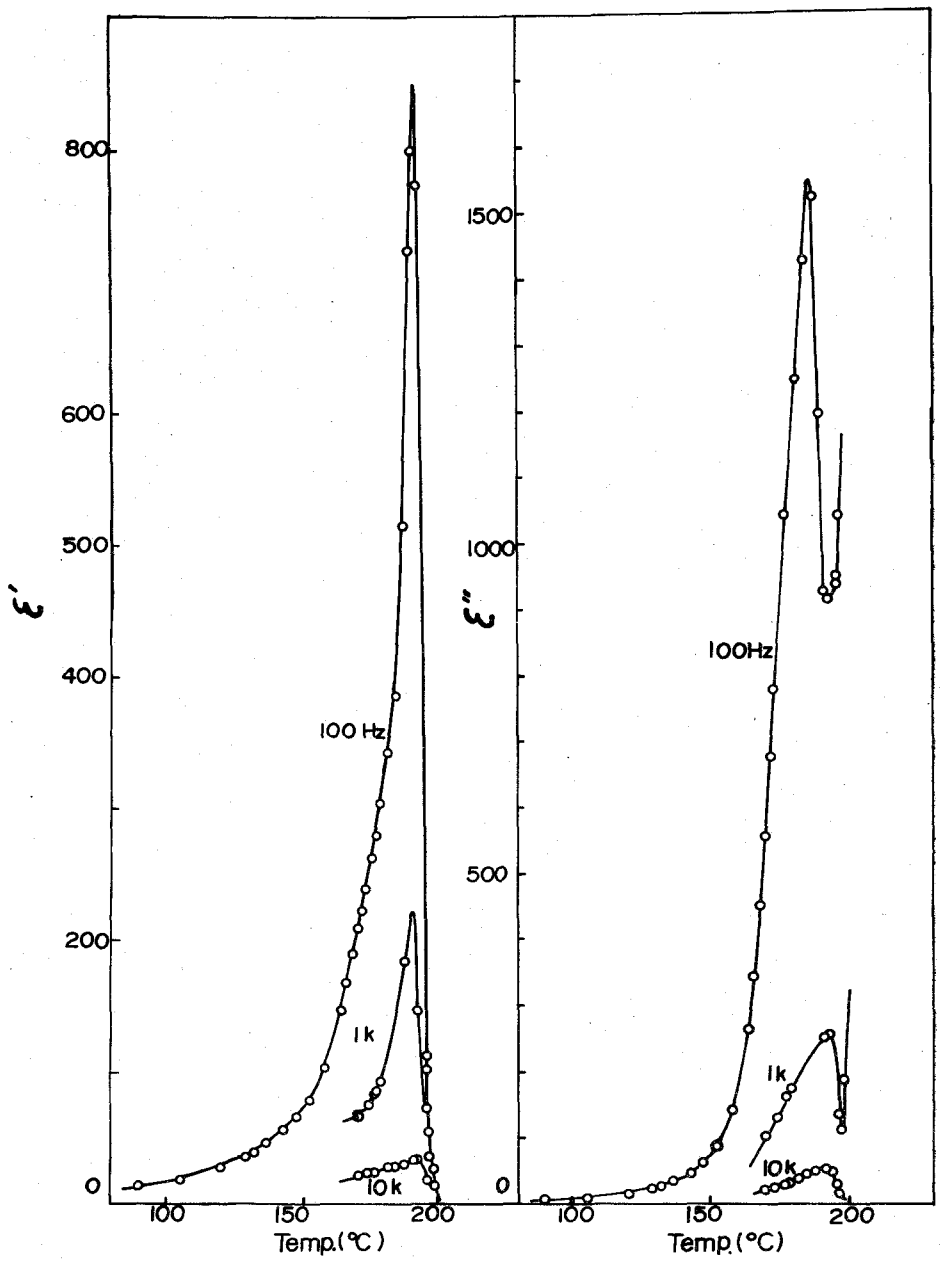

Fig. 5.1. Temperature dependence of ε' and ε" for a form III (ISO) specimen at various fixed frequencies.

attributable to ionic conduction, because it could be suppressed by applying a static electric field before dielectric measurement. Ions trapped in the crystalline portions should become mobile above the melting temperature and thus should cause an increase in ε''.

Figure 5.2 shows the frequency dependence of ε' and ε'' for form III (ISO) at 183°C, and Figure 5.3 presents the frequency dependence of ε'' for the same sample and a form II (MQ) sample at 165°C. It is seen that the ε'' curve for form III (ISO) is less steep than that for form II (MQ) and has a broad shoulder. Figure 5.4 shows the so-called transition map for form III (ISO); the open circles have been determined from the peaks in the ε'' versus temperature curves and the closed circle from the shoulder in the ε'' versus frequency curve at 183°C. The activation energy estimated from the indicated line is about 150 Kcal/mol.

We consider mechanisms responsible for the marked high temperature relaxation of form III PVDF.

(1) When form III (ISO) is melted and then cooled down to room temperature, form III crystals should be converted to form II crystals. In fact, the frequency dependence of ε' for a specimen obtained from the melt of a form III (ISO) specimen, which is displayed in Fig. 5.5, was almost identical to that of form II (MQ). Furthermore, a form III specimen did not show in its IR spectrum any absorption bands ascribable to thermal decomposition. These facts imply that the dielectric behavior in Figure 5.1 ought to be characteristic of form III PVDF itself.

(2) If this behavior were to arise from ionic impurities contained in the sample , it should be affected by application of a static electric field. However, the values of ε' measured under a dc bias was still as large as shown in Figure 5.1.

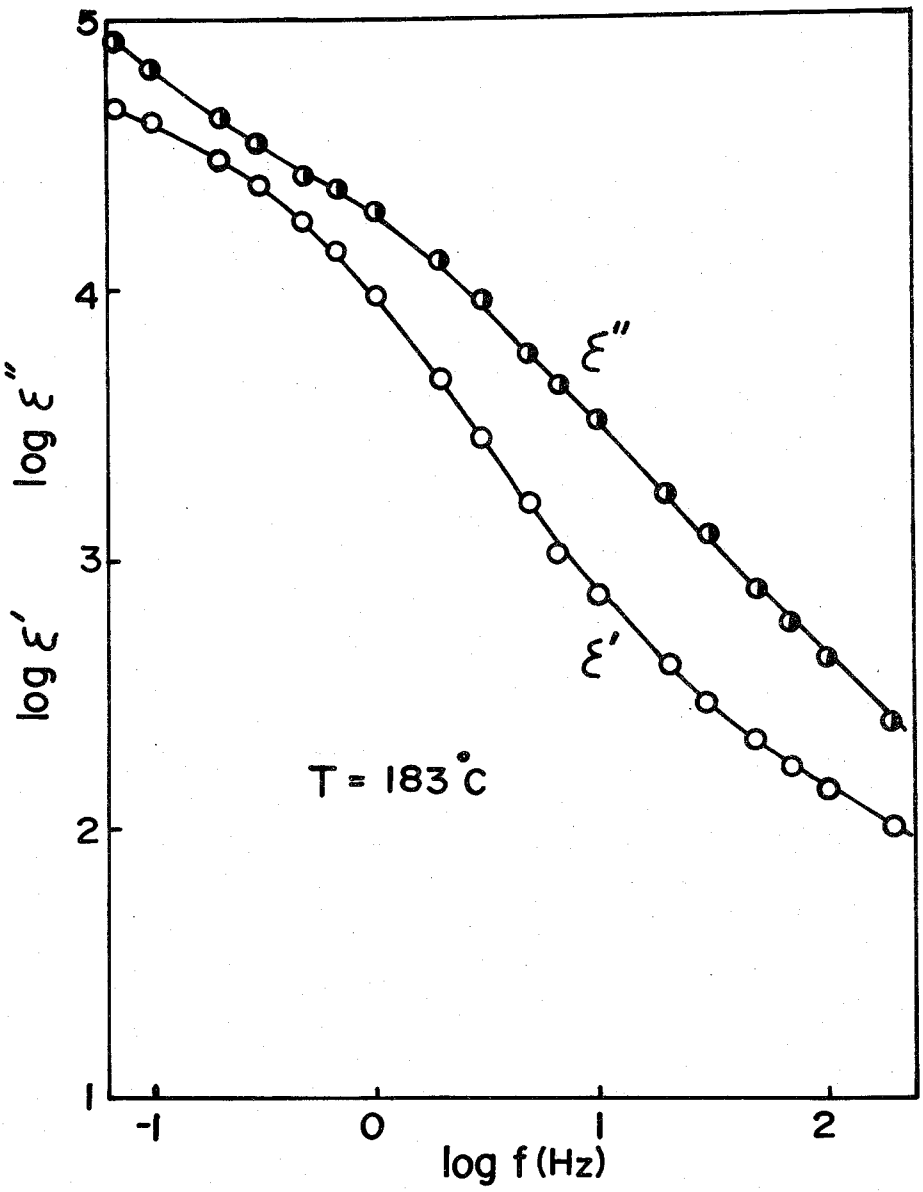

Fig. 5.2. Frequency dependence of ε' and ε" for a form III (ISO) specimen at 183°C.

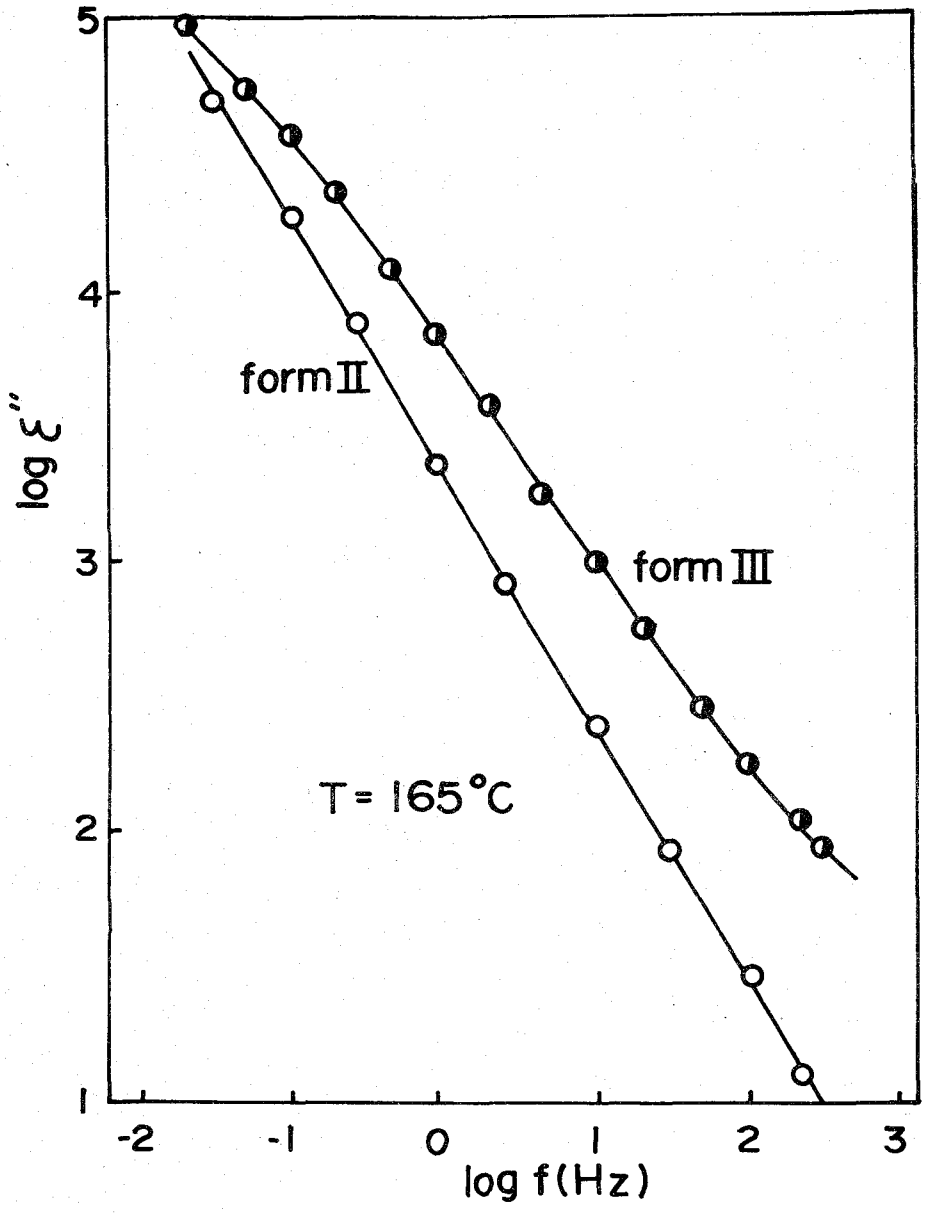

Fig. 5.3. Frequency dependence of ε'' for a form III (ISO) specimen and for a form II (MQ) specimen at 165°C.

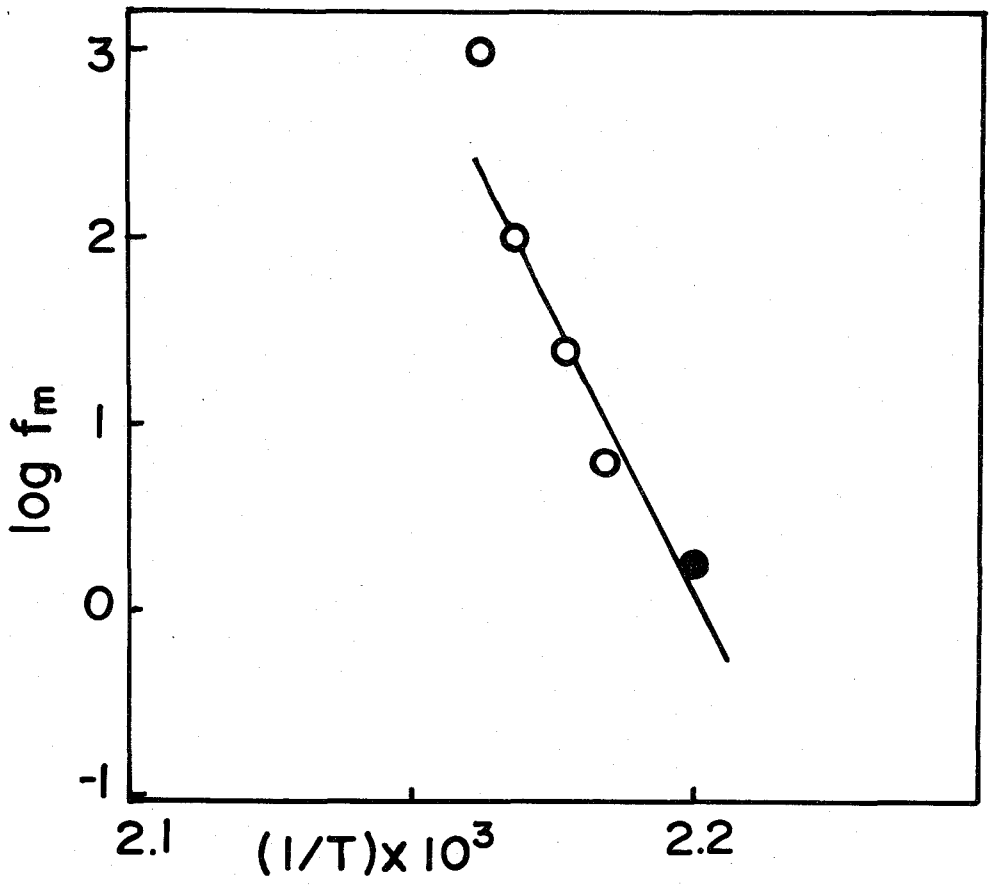

Fig. 5.4. Arrhenius plot for the high temperature relaxation of a form III PVDF specimen. The open circles were determined from the peaks in the ε'' versus temperature curves and the closed circle from the shoulder in the ε'' versus frequency curve at 183°C.

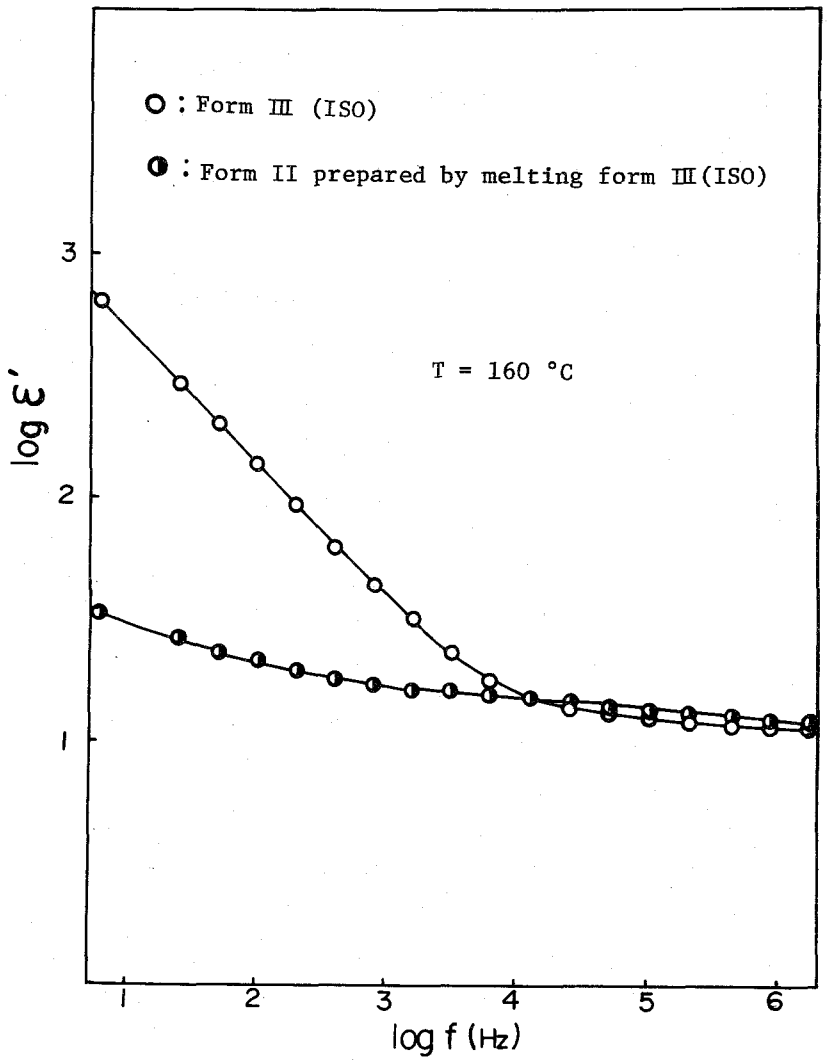

Fig. 5.5. Frequency dependence of ε' for a form III (ISO) specimen and for a form II (MQ) specimen prepared by melting a form III (ISO) specimen.

(3) A crystalline polymer is composed of crystalline and amorphous portions. According to the theory of inhomogeneous dielectrics, interfacial polarization should cause a dielectric dispersion. If we approximate the present system by a random suspension of isolated crystalline spheres of a dielectric constant ε_2 and an electric conductivity σ_2 immersed in an amorphous medium of a dielectric constant ε_1 and an electric conductivity σ_1, this effect should bring about a peak in ε'' at a frequency f given by[1]

$$f = 2(2\sigma_1 + \sigma_2)/(2\varepsilon_1 + \varepsilon_2)$$

Since, in actuality, $\sigma_1 >> \sigma_2$ and $\varepsilon_1 << \varepsilon_2$, this may be replaced by

$$f = 4\sigma_1/\varepsilon_2 \qquad (5\text{-}1)$$

When the electric conductivity σ of a form III (ISO) specimen at 185°C was measured with a dc voltage of 4×10^2 V/cm, σ reached a nearly constant value of 1.5×10^{-10} Ω^{-1} cm^{-1} after 15 hr, as shown in Figure 5.6. If this final value is used for σ_1 and the value of ε' at the peak for 100 Hz in Figure 5.1 is substituted for ε_2, equation (5-1) gives $f \simeq 0.6$ Hz, which is smaller than the expected frequency of 100 Hz by a factor of 2×10^2. This factor, though quite crude, is large enough to eliminate the possibility of attributing the behavior in Figure 5.1 to interfacial polarization.

(4) It has been shown in Chapter 2 that the high temperature peak observed near 200°C in the DSC thermogram of a form III (ISO) specimen is ascribed to the melting of form III crystals, and that the enthalpy H

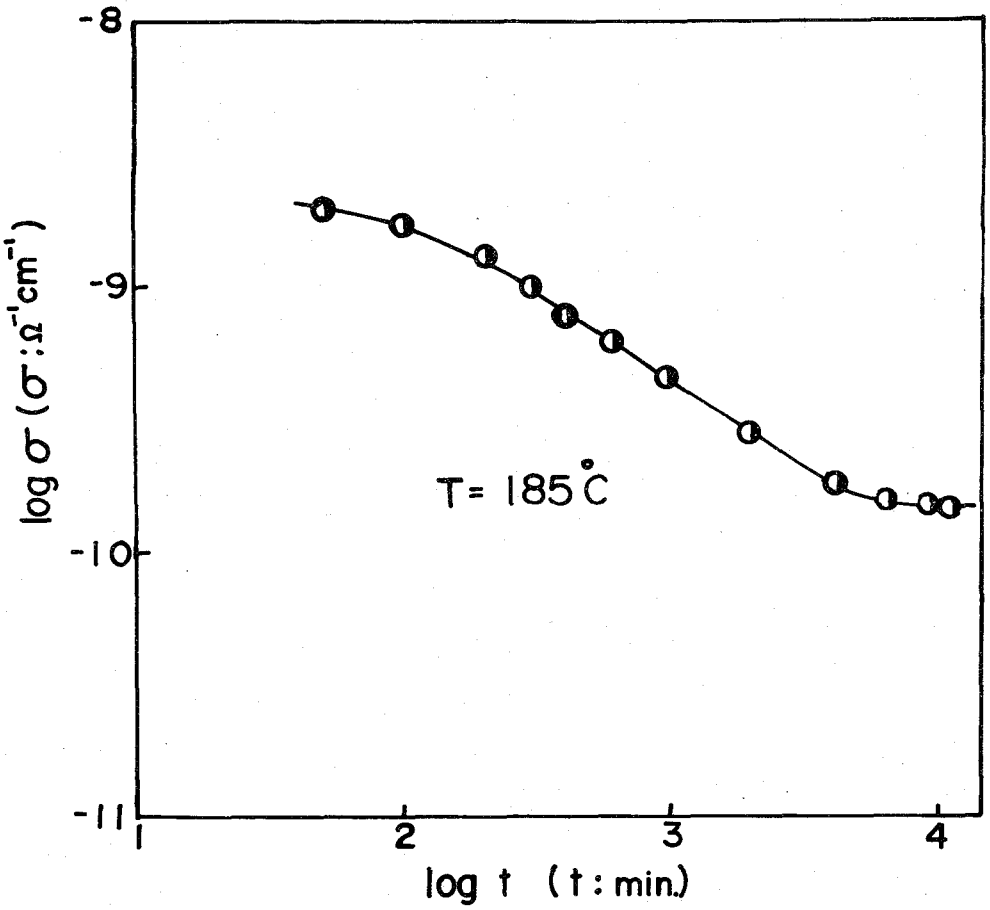

Fig. 5.6. Time dependence of electrical conductivity at 185°C for a form III (ISO) specimen.

associated with such a peak may be taken to be a measure of the amount of form III crystals at temperatures above 180°C. If the relaxation obeys a Debye type of equation, it follows that the relaxation strength $\Delta\varepsilon$ is proportional to ε''_{max}. Although this simple assumption apparently does not hold for the high temperature relaxation under consideration, we may regard ε''_{max} as a rough measure of $\Delta\varepsilon$. In Figure 5.7, ε''_{max} at 100 Hz for the high temperature relaxation curves of form III (ISO) samples crystallized at 167°C for different periods of time are plotted against H evaluated from the DSC curves of the corresponding samples. It is observed that ε''_{max} increases monotonically with H. This correlation suggests that form III crystals are mainly responsible for the marked high temperature dielectric dispersions as shown in Figure 5.1.

To obtain another support to this suggestion we tried to measure the mechanical loss of form III (ISO) at high temperatures, but the measurement encountered difficulties, because the specimen broke for partial melting of the crystalline portions. Hence we used form III (SVT) samples, since the ionic conduction which affected their dielectric behavior does not interfere with mechanical measurement. The results are illustrated in Figure 5.8. The peaks in loss modulus E'' are seen to shift to higher temperature as the long period of the crystal is increased. For form III (ISO) the loss peak would appear at a higher temperature than indicated here, probably at about 180°C, because such a sample is expected to have a long period reaching 140 - 150 Å. This expected peak temperature is comparable to the temperature for ε''_{max} in Figure 5.1. Such agreement, together with the fact that the feature of Figure 5.8 is similar to that reported for crystalline mechanical relaxation of solution-grown crystals

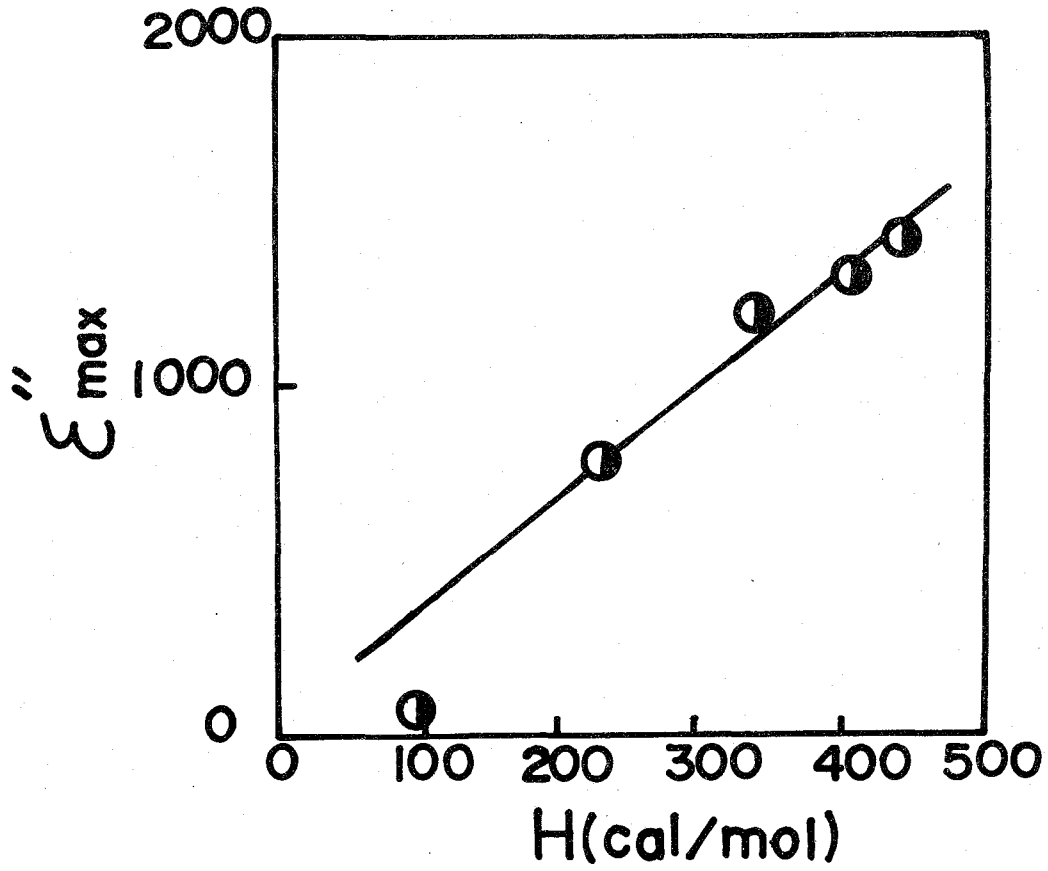

Fig. 5.7. Relationship between ε''_{max} at 100 Hz and eathalpy of fusion of form III crystals crystallized at 167°C for different times.

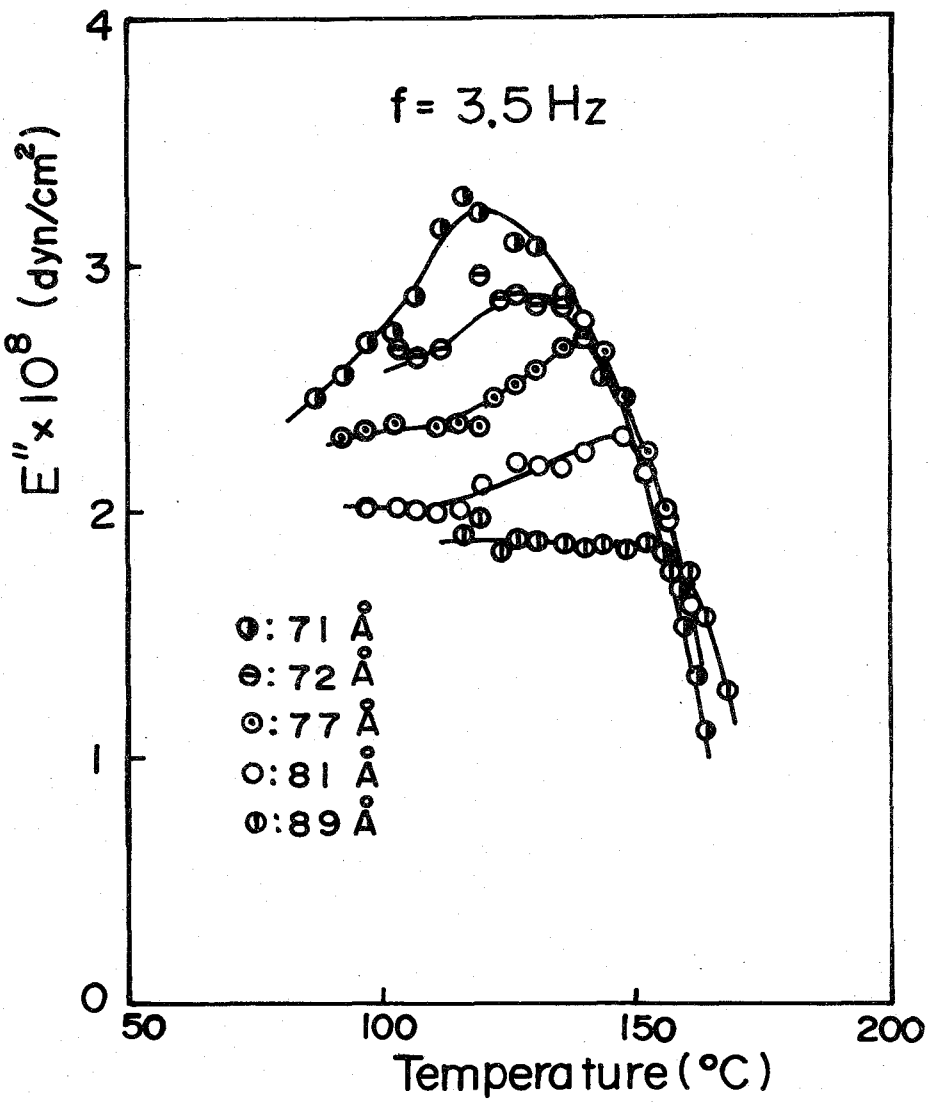

Fig. 5.8. Relationship between mechanical loss peak and long period for form III (SVT) sample. The long periods determined from small-angle X-ray photographs are given in the figure.

of polyethylene[3], suggests that the high temperature dielectric relaxation under consideration is an effect arising from the crystalline regions of form III PVDF.

However, the large strength of this relaxation can not be interpreted in terms of molecular motions associated with chain-folded lamellae. The peak value of ε'' at 100 Hz in Figure 5.1 is about 1400. This gives a relaxation strength of about 1.4×10^4 if a single relaxation mechanism is assumed. We now assume that n monomer units move cooperatively in a crystallite. Then n may be estimated from

$$\Delta\varepsilon = \frac{4\pi}{3}\left(\frac{E_r}{E}\right)\frac{N}{n}\frac{(n\mu)^2}{RT} \qquad (5\text{-}3)$$

where N is the number of monomer units per cm^3, μ is the dipole moment of a monomer unit, k is the Boltzmann constant, T is the absolute temperature, E is the applied electric field, and E_r is the local electric field. If we assume that $N \simeq 1.8 \times 10^{22}$, $\mu \simeq 2.1$ D, $T = 456°K$, and $E_r/E \simeq 1$, we find $n \simeq 3 \times 10^3$ for $\Delta\varepsilon = 1.4 \times 10^4$. Still larger values of n will be obtained if effects of crystallinity on $\Delta\varepsilon$ are taken into account and they are too large to be acceptable physically, because the ordinary lamellar thickness is several hundred Å, i.e. $n \sim 10^2$.

Thus, we finally reach the following two possibilites.

(5) Form III crystallites are polar. Therefore, they as a whole may undergo orientational motions with small amplitudes when an ac electric field is applied to the specimen. This idea is not inconsistent with large value of n obtained above. However, for rotational motions of

crystallites as a whole, the factor kT that appeared in equation (5-3) must be replaced by a rotational energy. This energy is to be larger than kT, because the rotation of a crystallite may not be regarded as free thermal motion. Thus, even a larger value of n is obtained when this replacement is made in equation (5-9)

To check the possibility of the orientational motion of form III crystallites, we measured the dielectric polarization of a form III (ISO) specimen as a function of ac electric field. The results are shown in Figure 5.9, from which the saturation polarization at 0.1 Hz and 185°C is estimated to be 9.5×10^5 coul./cm^2. This value is larger than the one expected when all crystallites undergo complete orientation, and hence it should contain some other contributions. The saturation polarization did not decrease much when a dc electric bias of 15 KV/cm was applied for 20 hr before measurement. The coercive electric field for the saturation curve is of the order of 100 KV/cm, which may be compared with the value obtained by Tamura et al.[4] for form I PVDF at room temperature.

Thus, the orientational motion of crystallites accompanying the applied ac electric field may be one of the most plausible mechanisms responsible for the marked dielectric dispersions of form III PVDF at high temperatures.

(6) Besides the orientation of crystalline regions, we can consider another possibility for the origin of the hysteresis loops shown in Figure 5.9. It is the existence of ferroelectric domains in form III crystallites. Each of such domains may have a large spontaneous polarization, and the motion of domain walls may bring about a hysteresis on the

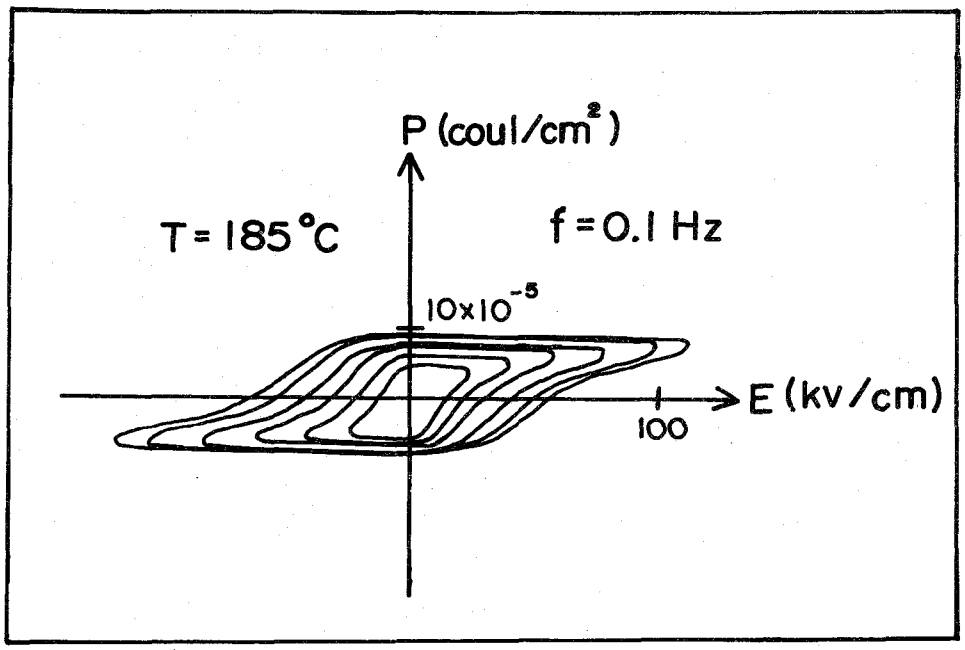

Fig. 5.9. P-E hysteresis loop for a form III (ISO) specimen.

polarization-electric field diagram. If this is the case, the value of n estimated above may be a little smaller than the actual number of monomer units contained in each form III crystallite. However, at present, it is difficult to detect experimentally the existence of ferroelectric domains in polymer crystals, and the above-mentioned possibility remains speculative.

References

1. K. W. Wagner, Arch. F. Elektrotechn., 2, 371, 374, 383 (1914).
2. Y. Wada, "The Physical Properties of Polymer Solids", Baifukan, Tokyo (1971).
3. M. Takayanagi and T. Matsuo, J. Macromol. Sci. Phys., B1(3), 407 (1967).
4. M. Tamura, K. Ogasawara, N. Ono, and S. Hagiwara, J. Appl. Phys., 45, 3768 (1974).

Chapter 6

Summary and Conclusions

This thesis has dealt with the following subject: conditions for preparing form II PVDF and form III PVDF and their dielectric behavior at high temperatures. Emphasis was put on the method for preparing form III (ISO) specimens suitable for dielectric measurements, the method for suppressing the ionic contribution to the complex dielectric constant, and the high temperature relaxation processes related to the crystalline regions in form II and form III specimens. The principal results are as follows.

(1) Optimum conditions for preparing form III (ISO) specimens appropriate for dielectric measurements were established by infrared spectroscopy, differential scanning calorimetry, and X-ray diffraction measurements. Form III was easily obtained by annealing form II (SGC) at temperatures between 175 and 185°C and preferentially formed by isothermal crystallization of the melt at temperatures between 165 and 175°C. Below 165°C crystallization of form II was formed. The melting point of form III was higher than that of form II.

(2) Dielectric measurements on form II (MQ) specimens at higher temperatures gave anomalously large values of ε' and ε'' at lower frequencies. When a static field was applied, a drastic decrease of ε' and ε'' occurred. The effects of a static field can be summarized as follows: (1) the field effects upon ε' and ε'' are more significant at

lower frequencies; (2) with increasing field strength, the rate of decrease in ε' and ε'' with time becomes greater; (3) when the field is removed, ε' and ε'' recover but the ultimate recovery is incomplete; (4) the field effect dependes strongly on temperature. These features seemed attributable to the displacement of ionic impurities and their electrolysis. In fact, this idea was confirmed by forced injection of ions into PVDF film by a high static field. The deposition of cations on the cathode was identified by emission spectroscopy. Application of a static electric field suppresses the contribution of ionic impurities to ε' and ε'' and thereby reveals the relaxation process of the polymer itself.

(3) In order to make clear whether the high temperature relaxation of form II PVDF is due to the crystalline or amorphous region, measurements were carried out with a form II (SGC) specimen. The strength of the observed high temperature relaxation was much larger than that of the form II (MQ) specimen. The relaxation disappeared suddenly above the melting point. These results were taken to indicate that the high temperature relaxation of form II arises from the crystalline region.

(4) Dielectric measurements on form III (ISO) specimens prepared by isothermal crystallization exhibited a marked relaxation at high temperatures near the melting point. The relaxation strength increased with increasing crystallinity, which suggested that the high relaxation is related to form III crystallites. The possibility of interfacial polarization for this relaxation was found to be eliminated from a comparison between calculated and observed frequencies for the maximum in the

dielectric loss curve. The "crystalline relaxation" due to molecular motions associated with the chain-folded lamellae was unable to account for the large relaxation strength. Finally, the following two possibilities were proposed: (a) the rotational motion of form III crystallites as a whole, in which almost all the dipoles are aligned in one direction, and (b) the motion of ferroelectric domains in form III crystallites. Although the mechanism (a) seems to be more probable, we cannot ignore the mechanism (b) at the present stage.

List of Publications

I. Part of the thesis has been published in

1. Effects of a Static Electric Field upon Dielectric Properties of Poly(vinylidene Fluoride) and Poly(vinyl Fluoride).
   S. Osaki, S. Uemura, and Y. Ishida, J. Polym. Sci., A-2, 9, 585 (1971).
2. Injection of Metal Ions into Polymer Film by an Electric Field.
   S. Osaki and Y. Ishida, J. Polym. Sci., A-2, 11, 801 (1973).
3. Dielectric Behavior of Poly(vinylidene Fluoride) in the Melt and in the Solution-Grown Crystal Mat.
   S. Osaki and Y. Ishida, J. Polym. Sci., A-2, 12, 1727 (1974).
4. Effects of Annealing and Isothermal Crystallization upon Crystalline Forms of Poly(vinylidene Fluoride).
   S. Osaki and Y. Ishida, J. Polym. Sci., Polym. Phys. Ed., 13, 1071 (1975).

II. List of related papers.

1. DC Bias Effects on Dielectric Constant and Loss Factor in Solid Polymers.
   S. Osaki, S. Uemura, and Y. Ishida, Rep. Progr. Polym. Phys. Japan, 8, 403 (1970).
2. Effects of a Static Electric Field upon Dielectric Properties of Poly(ε-caprolactam).
   S. Osaki, S. Uemura, and Y. Ishida, J. Polym. Sci., A-2, 9, 2099 (1971).